

1 **Soil water retention and hydraulic conductivity measured in a wide**
2 **saturation range**

3 Tobias L. Hohenbrink^{1,2}, Conrad Jackisch^{2,3}, Jackisch^{3,4}, Wolfgang Durner¹, Kai Germer^{1,4,5}, Sascha C. Iden¹,
4 Janis Kreiselmeier^{5,6}, Kreiselmeier^{6,7}, Frederic Leuther^{7,8}, Leuther^{8,9}, Johanna C. Metzger^{9,10}, Metzger^{10,11}, Mahyar
5 Naseri^{1,4,5}, Andre Peters¹

6 ¹ Institute of Geocology, Soil Science & Soil Physics, TU Braunschweig, Braunschweig, 38106, Germany

7 ^{2,2} Deutscher Wetterdienst (DWD), Agrometeorological Research Center, Braunschweig, 38116, Germany

8 ³ Interdisciplinary Environmental Research Centre, TU Bergakademie Freiberg, Freiberg, 09599, Germany

9 ^{4,4} Institute for Water and River Basin Management, Chair of Hydrology, Karlsruhe Institute of Technology (KIT), Karlsruhe,
10 76131, Germany

11 ^{4,5} Thünen Institute of Agricultural Technology, Braunschweig, 38116, Germany

12 ^{5,6} Thünen Institute of Forest Ecosystems, Eberswalde, 16225, Germany

13 ^{6,7} Institute of Soil Science and Site Ecology, TU Dresden, Tharandt, 01737, Germany

14 ^{7,8} Helmholtz Centre for Environmental Research - UFZ, Department of Soil System Sciences, Halle (Saale), 06120, Germany

15 ^{8,9} Department of Soil and Environment, Swedish University of Agricultural Sciences, Uppsala, 75007,
16 Sweden Bayreuth, 95447 Bayreuth, Germany

17 ^{9,10} Institute of Soil Science, Center for Earth System Research and Sustainability (CEN), Universität Hamburg, Hamburg,
18 20146, Germany

19 ^{10,11} Institute of Geoscience, Group of Ecohydrology, Friedrich Schiller University Jena, Jena, 07749, Germany

22 *Correspondence to:* Tobias L. Hohenbrink (t.hohenbrink@tu-braunschweig.de)

23 **Abstract.** Soil hydraulic properties (SHP), particularly soil water retention capacity and hydraulic conductivity of unsaturated
24 soils, are among the key properties that determine the hydrological functioning of terrestrial systems. Some large collections
25 of SHP, such as the UNSODA and HYPRES databases, already exist for more than two decades. They have provided an
26 essential basis for many studies related to the critical zone. Today, sample-based SHP can be determined in a wider saturation
27 range and with higher resolution by combining some recently developed laboratory methods. We provide 572 high-quality
28 SHP data sets from undisturbed, mostly central European samples covering a wide range of soil texture, bulk density and
29 organic carbon content. A consistent and rigorous quality filtering ensured ensures that only trustworthy data sets were
30 included. The data collection contains: (i) SHP data: soil water retention and hydraulic conductivity data, determined by the
31 evaporation method and supplemented by retention data obtained by the dew point method and saturated conductivity
32 measurements, (ii) basic soil data: particle size distribution determined by sedimentation analysis and wet sieving, bulk density
33 and organic carbon content, as well as (iii) meta data metadata including the coordinates of the sampling locations. In addition,
34 for each data set, we provide soil hydraulic parameters for the widely used van Genuchten-Mualem model and for the more

| | |
|--------------------------|------|
| Formatvorlagendefinition | [9] |
| Formatvorlagendefinition | [8] |
| Formatvorlagendefinition | [7] |
| Formatvorlagendefinition | [6] |
| Formatvorlagendefinition | [5] |
| Formatvorlagendefinition | [4] |
| Formatvorlagendefinition | [3] |
| Formatiert | [12] |
| Formatiert | [10] |
| Formatiert | [11] |
| Formatiert | [13] |
| Formatiert | [14] |
| Formatiert | [15] |
| Formatiert | [16] |
| Formatiert | [17] |
| Formatiert | [18] |
| Formatiert | [19] |
| Formatiert | [20] |
| Formatiert | [21] |
| Formatiert | [22] |
| Formatiert | [23] |
| Formatiert | [24] |
| Formatiert | [25] |
| Formatiert | [26] |
| Formatiert | [27] |
| Formatiert | [28] |
| Formatiert | [29] |
| Formatiert | [30] |
| Formatiert | [31] |
| Formatiert | [32] |
| Formatiert | [33] |
| Formatiert | [34] |
| Formatiert | [35] |
| Formatiert | [36] |
| Formatiert | [37] |
| Formatiert | [38] |
| Formatiert | [39] |
| Formatiert | [40] |
| Formatiert | [1] |
| Formatiert | [2] |

35 [advanced](#) Peters-Durner-Iden (PDI)-model, which accounts for non-capillary retention and conductivity. The data were
36 originally collected to develop and test [advaneedSHP](#) models-of SHP and associated pedotransfer functions. However, we
37 expect that they will be very valuable for various other purposes such as simulation studies or correlation analyses of different
38 soil properties to study their causal relationships. The data is available under the DOI link
39 <https://doi.org/10.5880/fidgeo.2023.012> (Hohenbrink et al., 2023; the final DOI will be registered before publication, please
40 use the review link meanwhile: <https://dataservices.gfz-potsdam.de/panmetaworks/review/5c617cd2664ea4d03e81301b5bc2236f1948a3cf7eb9bad48da940524f0cbac0>).

43 **1 Introduction**

44 A sound understanding of the hydrological functioning of variably-saturated soils in the environmental cycles is important for
45 numerous applications in agronomy, forestry, water management and other disciplines. The hydrological functioning of soils
46 is controlled by the soil hydraulic properties (SHP), specifically the water retention and hydraulic conductivity characteristics.
47 SHP models are essential to simulate water dynamics, solute transport and energy transfers in the vadose zone using water
48 flow and transport equations. Such SHP models are empirical mathematical representations of the highly non-linear soil
49 hydraulic curves, which are parameterised based on measured SHP data. In order to estimate SHP from more accessible
50 information, pedotransfer functions relate SHP parameters to basic soil properties like soil texture, bulk density, and organic
51 carbon content (C_{org}) (Vereecken et al., 2010; Van Looy et al., 2017).

52 Since the early applications of SHP models in hydrological simulations in the 1980s, there is a demand for such parameters
53 (Carsel and Parrish, 1988). Commonly, they are derived for specific SHP models (Vereecken et al., 2010), which is most often
54 the van Genuchten-Mualem model (Van Genuchten, 1980; Mualem, 1976). Fitting non-linear SHP models to observed data
55 and developing pedotransfer functions both require large data collections containing information about SHP measured over a
56 large range of saturation in samples with various combinations of basic soil properties. Such data collections are commonly
57 based on individual soil samples from various profiles.

58 Since the application of SHP models in hydrological simulations in the 1980s there is a demand for such parameters (Carsel
59 and Parrish, 1988). Commonly, they are derived for specific SHP models (Vereecken et al., 2010), which is most often the van
60 Genuchten Mualem model (Van Genuchten, 1980; Mualem, 1976). Due to methodological restrictions, data for such
61 applications were first limited to few points on the soil water retention curve using ceramic pressure plate extractors and
62 pressure-controlled hydraulic conductivity (Brooks and Corey, 1964).

63 Since the late 1990s, different data collections of SHP and associated basic soil properties have been compiled. They formed
64 the basis to develop various pedotransfer functions. The freely available Unsaturated Soil Hydraulic Database (UNSODA)
65 provided by the U.S. Department of Agriculture comprises nearly 800 SHP data sets from disturbed and undisturbed samples
66 (Nemes et al., 2001). It includes measurements of retention and hydraulic conductivity with different coverage of the saturation

Formatiert: Schriftart: Fett, Schriftfarbe: Schwarz

Formatiert: Standard, Abstand Vor: 24 Pt., Nach: 12 Pt.,
Nicht vom nächsten Absatz trennen, Rahmen: Oben: (Kein Rahmen), Unten: (Kein Rahmen), Links: (Kein Rahmen),
Rechts: (Kein Rahmen), Zwischen : (Kein Rahmen)

Formatiert: Schriftfarbe: Schwarz

Formatiert: Standard, Rahmen: Oben: (Kein Rahmen),
Unten: (Kein Rahmen), Links: (Kein Rahmen), Rechts: (Kein Rahmen), Zwischen : (Kein Rahmen), Tabstopps: 7,96 cm,
Zentriert + 15,92 cm, Rechtsbündig

67 range as well as basic soil properties, e.g. information on soil texture or bulk density. UNSODA was an important basis to
68 develop ROSETTA (Schaap et al., 2001; Zhang and Schaap, 2017), which is the most established pedotransfer function to
69 predict the parameters of the van Genuchten-Mualem SHP model.

70 Another prominent large collection of retention and hydraulic conductivity data is the database of the Hydraulic Properties of
71 European Soils (HYPRES) (Wosten et al., 1999) and its further development as the European Hydropedological Data Inventory
72 (EU-HYDI) (Weynants et al., 2013) which is unfortunately not freely available. There are a few more specific SHP data
73 collections, e.g. the HYBRAS data describing Brazilian tropical soils (Ottoni et al., 2018), and the collection by Schindler and
74 Müller (2017) which contains only data measured with the evaporation method (Peters and Durner, 2008; Schindler, 1980).
75 Recently, Gupta et al. (2022) gathered published soil water retention data from 2,702 sites, prepared them for an easy use in
76 land surface modeling and made them commonly openly accessible.

Formatiert: Englisch (Vereinigtes Königreich)

77 The existing databases have undoubtedly supported a large number of hydrological studies leading to important conclusions,
78 but they still have some limitations and shortcomings. Often, SHP data only cover a small part of the naturally occurring range
79 of soil saturation. Gupta et al. (2022) emphasised that in many cases the retention data series contain only a few pairs of data
80 and lack information in the wet region close to full saturation. Measured saturated hydraulic conductivity (K_{sat}) is included in
81 several data collections, but detailed information about the unsaturated hydraulic conductivity is still rare.

82 It is technically possible to create pedotransfer functions that using only use retention and K_{sat} data (Assouline and Or, 2013) as
83 has often been done in the past. However, in such cases the shape of the hydraulic conductivity curves is predicted only
84 from the water retention curve and scaled to match K_{sat} . Hence, the absolute position of the conductivity curve is solely
85 determined by a single K_{sat} value, which is strongly influenced by soil structure and macropore connectivity, which are often
86 not recorded nor assessed at the time of sampling.

87 A serious development and rigorous testing of full-range SHP models always requires measured unsaturated hydraulic
88 conductivity data. Zhang et al. (2022) showed impressively how fast a supposedly large number of available SHP data sets can
89 collapse, when they are filtered by predefined data requirements. They initially gathered 19,510 data sets from established data
90 collections and first narrowed it down to 14,997 data sets describing undisturbed samples. They then extracted 1,801 lab
91 measured data sets with information about both soil water retention and hydraulic conductivity. Finally, they extracted data
92 sets with at least six retention and seven conductivity data pairs, each of which contained at least three data pairs close to
93 saturation at matric heads larger than -20 cm. They ended up with 194 data sets accounting for only 1 % of the initial number.

94 Considering Given the largewide variability of naturally occurring soils, many pedotransfer functions are based on data
95 collections that comprisecontain rather limited soil information. Weihermüller et al. (2021) showed that the choice of the
96 pedotransfer function used in a soil hydrological model can have considerable effects on simulated water fluxes. The artificial
97 neural network behind ROSETTA has been trained with 2,134 retention curves, 1,306 K_{sat} values and 235 unsaturated
98 conductivity curves (Schaap et al., 2001; Zhang and Schaap, 2017). Considering the wide use of ROSETTA with more than
99 1,790,840 citations (retrieved from Scopus on 20/02/07/2023) it becomes apparent, that the specific characteristics of only 235
100 unsaturated hydraulic conductivity data sets have been propagated into a large number of applications and conclusions.

Formatiert: Englisch (Vereinigtes Königreich)

Formatiert: Schriftfarbe: Schwarz

Formatiert: Standard, Rahmen: Oben: (Kein Rahmen), Unten: (Kein Rahmen), Links: (Kein Rahmen), Rechts: (Kein Rahmen), Zwischen : (Kein Rahmen), Tabstopps: 7,96 cm, Zentriert + 15,92 cm, Rechtsbündig

101 However, pedotransfer functions can only predict the SHP within the range covered by the training dataset. Furthermore, they
102 tend to reflect the individual characteristics of the training data, which are most pronounced in case of small databases. To
103 prevent such **bottleneck** effects, the basis for pedotransfer applications needs to be further diversified. This requires
104 new and independent, quality-assured SHP data collections. With advanced measuring techniques becoming standard in many
105 soil physical laboratories, it is now much easier to obtain experimental SHP data over a wider range of **soil moisture content**
106 and in the desired high quality.

107 In this paper, we present a collection of 572 new data sets of soil properties **measured in soil samples** (Hohenbrink et al., 2023)
108 that are independent of existing databases. Each data set **comprises** (i) SHP, and (ii) **the basic soil properties such as**
109 soil texture, bulk density and C_{org} . The SHP data meet high quality requirements since they have been determined by combining
110 state-of-the-art laboratory techniques, i.e. **the evaporation method** (Peters and Durner, 2008; Schindler, 1980), **the dewpoint**
111 **methodpotentiometry** (Campbell et al., 2007), and separate K_{sat} measurements. In addition, each **data set was subjected to**
112 **a dataset has undergone** thorough quality control. The data collection covers a wide range of soil textures. **TheSoil** texture
113 information **on soil texture** is provided **on two levels: main texture groups inaccordance to both** the German (**Ad-hoc-**
114 **Arbeitsgruppe Boden, 2005**) and **the USDA classification system andsystems** (USDA, 1999). Within the silt and sand classes,
115 **we also provide** the sub-classes for silt and sand, respectively, coarse, medium and fine according to the German system.
116 In support of the FAIR principles (Wilkinson et al., 2016), we **would like to** provide free access to **this strong foundation for**
117 **developing powerful the data for the development of** SHP models and pedotransfer functions. **The data were originally**
118 **collected to provide a basis for the development of advanced SHP models** (Peters et al., 2021, 2023) and related pedotransfer
119 **functions**. We expect **that they will them to** be valuable for **various furthera variety of** purposes such as simulation studies and
120 statistical analyses of various soil properties.

121 **2 Materials and Methods**

122 **2.1 Data sources**

123 **The data sets originate from different laboratories and have been collected for various original purposes. After launching aA**
124 **community initiative for collecting and sharing consistent SHP data setswas launched by researchers from** the Division of Soil
125 **Science and Soil Physics at TU Braunschweig, researchers, Scientists** from four **other** institutions participated **and provided**
126 **databy providing data measured in their laboratories**. Most of the data had already been used to answer individual research
127 questions at various research sites (Jackisch et al., 2017; Kreiselmeier et al., 2019, 2020; Leuther et al., 2019; Jackisch et al.,
128 2020; Germer and Braun, 2019; Metzger et al., 2021). **Further alreadySome** existing but yet unpublished data sets **measured**
129 **at TU Braunschweig** have been reviewed and integrated into the data collection, **too**. In addition, we systematically added data
130 from sites with soil characteristics that were missing from the data collection. **We took soil samples at these sites and measured**
131 **their propertiesSuch data were explicitly measured** for this data collection.

Formatiert: Schriftfarbe: Schwarz

Formatiert: Schriftart: Fett, Schriftfarbe: Schwarz

Formatiert: Standard, Abstand Vor: 24 Pt., Nach: 12 Pt.,
Nicht vom nächsten Absatz trennen, Rahmen: Oben: (Kein Rahmen), Unten: (Kein Rahmen), Links: (Kein Rahmen),
Rechts: (Kein Rahmen), Zwischen : (Kein Rahmen)

Formatiert: Schriftart: Fett, Schriftfarbe: Schwarz

Formatiert: Schriftfarbe: Schwarz

Formatiert: Englisch (Vereinigtes Königreich)

Formatiert: Schriftfarbe: Schwarz

Formatiert: Standard, Rahmen: Oben: (Kein Rahmen),
Unten: (Kein Rahmen), Links: (Kein Rahmen), Rechts: (Kein Rahmen), Zwischen : (Kein Rahmen), Tabstopps: 7,96 cm,
Zentriert + 15,92 cm, Rechtsbündig

132 To select data sets meeting our standards and optimally covering (a) soil texture, (b) bulk density, and (e) C_{org} be included in
133 the data collection, the data sets must had to contain soil water retention and hydraulic conductivity data, measured in the
134 laboratory by the evaporation method, preferably supplemented by dewpoint method data and also measurements of saturated
135 hydraulic conductivity. The data sets should also had to include information about soil texture, and bulk density, and preferably
136 C_{org} . WeWe have aimed to cover the data space of these basic soil properties as completely as possible. Therefore, we also
137 included data sets that lacked some of the preferred information only if, when they added complementarynew combinations of
138 basic soil properties to the data collection.

139 2.2 Soil samples

140 Each data set is based on one undisturbed soil sample taken in situ with metal cylinders. In 542 cases the sample volume was
141 250 cm³, while 30 samples had a volume of 692 cm³ as indicated in the meta-data metadata table of Hohenbrink et al. (2023).
142 For the measurement of C_{org} , soil texture and retention data in the dry range (dewpoint method), disturbed soil (sub)samples
143 were taken. In 363 cases, the exactly one disturbed and undisturbed samples are directly sample was assigned to each
144 otherundisturbed sample, either by taking theboth samples in immediateclose proximity to each other, or by taking the
145 disturbed sample directly from the undisturbed sample material after measuring the SHP. In the other 209 cases, the disturbed
146 materialsample was taken as a-mixed samplematerial, representative effor an entire site with several undisturbed sampling
147 points. Consequently, in the latter cases the soil variables derived from the aggregated undisturbeddisturbed samples have been
148 assigned to more than one data set (indicated in the meta-data metadata table). Information about the positions of the sampling
149 sites is available for 555 data sets. It has either been measured by GPS or was taken from aerial images after sampling. The
150 geo-positions are reported with a lateral accuracy of the reported sampling locations is smaller than 100 m, which represents
151 the best accuracy class in Gupta et al. (2022). The sampling depth is reported for 474 samples in the metadata table.

152 2.3 Laboratory measurements

153 Soil water retention in the wet (defined here as $pF < 1.8$; $pF = \log_{10}(-h [cm])$) and medium (defined
154 here as $1.8 < pF < 4.2$) moisture range and hydraulic conductivity in the medium moisture range were simultaneously
155 determined with the simplified evaporation method (Peters and Durner, 2008; Schindler, 1980) using the HYPROP device
156 (METER Group, AG, Germany). The evaporation method provides information related to the drying branches of the SHP
157 curves. The air entry points of the tensiometer cups have beenwere used as an additional measuring point (Schindler et al.,
158 2010) in cases where the duration of the evaporation experiments was long enough. Soil water retention information has
159 beenwas supplemented mainly in the dry moisture range (defined here as $pF > 4.2$) by measurements with the dewpoint method
160 (Campbell et al., 2007; Kirste et al., 2019) using the WP4C device (METER Group, Inc., USA). Hydraulic conductivity of the
161 saturated soil was measured in the undisturbed samples either with the falling head or the constant head method using the
162 KSAT device (METER Group, AG, Germany).

Formatiert: Schriftart: Fett, Schriftfarbe: Schwarz

Formatiert: Standard, Abstand Vor: 12 Pt., Nach: 12 Pt., Mit Gliederung + Ebene: 2 + Nummerierungsformatvorlage: 1, 2, 3, ... + Beginnen bei: 2 + Ausrichtung: Links + Ausgerichtet an: 0 cm + Einzug bei: 0,63 cm, Nicht vom nächsten Absatz trennen, Rahmen: Oben: (Kein Rahmen), Unten: (Kein Rahmen), Links: (Kein Rahmen), Rechts: (Kein Rahmen), Zwischen : (Kein Rahmen)

Formatiert: Schriftfarbe: Schwarz

Formatiert: Schriftart: Fett, Schriftfarbe: Schwarz

Formatiert: Schriftfarbe: Schwarz

Formatiert: Standard, Abstand Vor: 12 Pt., Nach: 12 Pt., Nicht vom nächsten Absatz trennen, Rahmen: Oben: (Kein Rahmen), Unten: (Kein Rahmen), Links: (Kein Rahmen), Rechts: (Kein Rahmen), Zwischen : (Kein Rahmen)

Formatiert: Schriftfarbe: Schwarz

Formatiert: Standard, Rahmen: Oben: (Kein Rahmen), Unten: (Kein Rahmen), Links: (Kein Rahmen), Rechts: (Kein Rahmen), Zwischen : (Kein Rahmen), Tabstopps: 7,96 cm, Zentriert + 15,92 cm, Rechtsbündig

163 Particle size distributions of the disturbed soil samples ~~have been~~were determined by wet sieving for the sand fractions and
164 sedimentation methods for the silt fractions and clay content (DIN ISO 11277, 2002). ~~The~~ Since the data sets originate from various
165 sources, the The sedimentation analyses ~~have been performed following~~were carried out with slightly different approaches in
166 each lab protocols, which, however, are all based on the same principles. Limits between ~~as~~ specified for each dataset in the
167 metadata table. The respective particle size classes were defined by the German soil classification system (Ad-hoc-
168 Arbeitsgruppe Boden, 2005) and afterwards additionally converted to the USDA system). Because the German system differs
169 from international standards in the boundary between silt and sand (German: 63 µm, USDA: 50 µm) we additionally converted
170 the texture data by interpolation with monotone cubic splines fitted to the cumulative particle size distributions as
171 recommended by Nemes et al. (1999). Illustrations showing data in the texture triangle were created using the “soiltexture” R-
172 package (Moeys, 2018). Bulk density of each sample was determined by oven-drying for at least 24 h after the evaporation
173 experiments. C_{org} was determined with high-temperature combustion using different elemental analysers (indicated, which are
174 listed in the meta-data table).

Formatiert: Englisch (Vereinigtes Königreich)

2.4 Fitting models to measured SHP data

2.4 Data preparation and quality check

The results of all SHP measurements have been compiled with the HYPROP-FIT software (Pertassek et al., 2015), a software).
It was developed to organize and evaluate raw data from the simplified evaporation method, the dewpoint method and individual K_{sat} measurements. Since
Despite a high level of automation and standardisation, manual adjustments to selecting the raw data for evaluation is required.
To avoid misalignment due to differences in the manual treatment, all resulting retention and hydraulic conductivity points
have been re-checked for plausibility by the same expert based on the following procedure:

1. Tensiometer check and offset correction: HYPROP uses two tensiometers at different levels. If in the first hours of the experiments (close to saturation) the measured difference between the upper and lower tensiometers deviate from the actual difference of 2.5 cm by more than 1 cm, an offset correction was performed to prevent unrealistic hydraulic gradients during data evaluation.
2. Consistency check if the initial water content was smaller than the porosity: If not, a slightly larger column height (1 - 4 mm) has been assumed to account for consistency. In a few cases, individual dewpoint surplus water in the data evaluation.
3. Setting the evaluation limits of the evaporation method: Because not all measurements that were clearly inconsistent follow idealistic conditions, the data for evaluation have been limited to plausible records (capillary connection of the tensiometers, plausible upward gradient, omission of scattered values for unsaturated conductivity near saturation).

Formatiert: Schriftfarbe: Schwarz

Formatiert: Standard, Rahmen: Oben: (Kein Rahmen), Unten: (Kein Rahmen), Links: (Kein Rahmen), Rechts: (Kein Rahmen), Zwischen : (Kein Rahmen), Tabstopps: 7,96 cm, Zentriert + 15,92 cm, Rechtsbündig

- 194 4. Omit retention data of the dewpoint potentiometry outside its validity limits: dewpoint potentiometry measurements
 195 tend to be less precise for lower tensions. To avoid unnecessary variance between the different methods (dewpoint
 196 and evaporation), values below pF 4 were omitted.
 197 5. Plausibility of hydraulic conductivity values: In cases of values for unsaturated conductivity exceeding the separately
 198 measured saturated conductivity, such values were omitted from the original sources.
 199 6. Visual alignment check for data from the three methods (K_{sat} , evaporation, dewpoint) and omission of obviously
 200 misaligned datasets from the collection.

201 The original binary HYPROP-FIT files are provided by Hohenbrink et al. (2023) to ensure transparency on all manual
 202 adjustments. The final series of measured retention and hydraulic conductivity data were exported from HYPROP-FIT to csv-
 203 files for further data processing, which was mainly performed in R (R Core Team, 2020).

204 **2.5 Fitting models to measured SHP data**

205 For direct access to resulting SHP model parameters, we fitted two models to the measured soil water retention and hydraulic
 206 conductivity data using a shuffled complex evolution (Duan et al., 1992) in SHYPFIT 2.0 (Peters and Durner, 2015). The first
 207 model is the well-established van Genuchten-Mualem (VGM) model (Van Genuchten, 1980; Mualem, 1976). The second
 208 model is the recent version of the Peters-Durner-Iden (PDI) model with the VGM model as the basic function (Peters et al.,
 209 2021, 2023).

210 The PDI model specifically considers (i) capillary water in completely filled pores and (ii) non-capillary water in thin films on
 211 particle surfaces and in corners and ducts of the pore system. The explicit consideration of non-capillary water yields more
 212 realistic retention and hydraulic conductivity curves in the medium and dry moisture range. Furthermore, the description of
 213 hydraulic conductivity in the dry range includes an effective component that reflects isothermal vapour flux (Peters, 2013).
 214 Unlike VGM and common models of SHP, where the relative hydraulic conductivity curve is sealed by the saturated
 215 conductivity K_s , the new PDI model structure allows absolute conductivity prediction based on the water retention curve. This
 216 enables a more realistic conductivity prediction under nearly saturated conditions (Peters et al., 2023). Additionally, we
 217 constrained the conductivity model by a maximum pore radius close to saturation, referring to an equivalent water tension of
 218 $h = -6 \text{ cm}$ (Iden et al., 2015). We refer to Peters et al. (2023) for a more detailed description of the applied version of the PDI
 219 model.

220 Retention and conductivity parameters were estimated simultaneously. RetentionDuring model fitting the few retention points
 221 measured with the dewpoint method were weighted ten times higher than those obtained with the evaporation method because
 222 the latter have a much higher frequency. Weights of hydraulic conductivity data were defined in a way that their
 223 ratio to the mean retention data weights was 16 to 10,000 following Peters (2013). We neglected measured K_{sat} values in the
 224 parameter optimization process, since they mainly reflect effects of soil structure (Weynants et al., 2009), which is not

Formatiert: Schriftfarbe: Schwarz

Formatiert: Standard, Rahmen: Oben: (Kein Rahmen), Unten: (Kein Rahmen), Links: (Kein Rahmen), Rechts: (Kein Rahmen), Zwischen : (Kein Rahmen), Tabstopps: 7,96 cm, Zentriert + 15,92 cm, Rechtsbündig

225 considered in the unimodal SHP models. The saturated hydraulic conductivity model parameter K_s equals the hydraulic
226 conductivity of the saturated bulk soil excluding the soil macropore network.

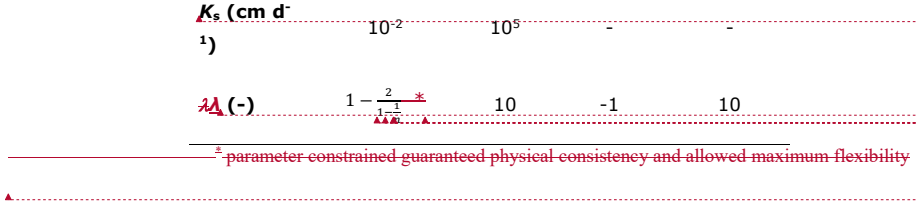
227 For the VGM model six parameters were estimated (residual and saturation water contentscontent θ_r (-) and θ_s (-), the shape
228 parameters α (cm^{-1}) and n (-), the tortuosity parameter λ (-), and the saturated hydraulic conductivity parameter K_s (cm d^{-1})).
229 The predefined parameter limits are listed in Table 1. The upper limits for θ_r and θ_s were defined as a fraction of porosity Φ to
230 ensure physical consistency. For the PDI model, five parameters (θ_r , θ_s , α , n and λ) were estimated. The with the same
231 settings for the and fitting algorithms as in Peters et al. (2023) were used. The parameter K_s in the PDI frame was calculated
232 from the water retention curve and equals the hydraulic conductivity of the saturated bulk soil excluding the soil macropore
233 network.).

234 Unlike VGM and common models of SHP, where the relative hydraulic conductivity curve is scaled by the saturated
235 conductivity K_s , the new PDI model structure allows to realistically predict conductivity data close to saturation, which are
236 usually not available (Peters et al., 2023). To avoid an unrealistically sharp drop of the conductivity curve close to saturation
237 for soils with wide pore size distribution, we constrained the conductivity model by a maximum pore radius (maximum tension)
238 close to saturation with the “h-clip approach” (Iden et al., 2015).

239 According to Jarvis (2007), the maximum tension was set to -6 cm (5 mm equivalent pore diameter). The saturated conductivity
240 is defined as the predicted absolute conductivity at this tension. We refer to Peters et al. (2021, 2023) for a more detailed
241 description of the applied version of the PDI model.

242 **Table 1: Upper and lower parameter boundaries defined for fitting the van Genuchten-Mualem model (VGM) and the Peters-
243 Durner-Iden model (PDI). α and n : shape parameters, θ_r and θ_s : residual and saturation water content, K_s : saturated hydraulic
244 conductivity parameter estimation, λ : tortuosity parameter. Note that the parameter boundaries for θ_r and θ_s are defined
245 individually as a fraction of the porosity Φ . The boundaries for θ_r and λ differ between both models to ensure physical consistency.
246 The lower λ constraint for VGM is set to guarantee physical consistency while allowing for maximum flexibility.**

| | VGM | | PDI | |
|-------------------------------|-----------|-------------------|-----------|-------------------|
| | lower | upper | lower | upper |
| α (cm^{-1}) | 10^{-5} | 0.5 | 10^{-5} | 0.5 |
| n (-) | 1.01 | 8.00 | 1.01 | 8.00 |
| $\theta_r \theta_s$ (-) | 0.0 | $0.25 \cdot \Phi$ | 0.0 | $0.75 \cdot \Phi$ |
| θ_s (-) | 0.2 | Φ | 0.2 | Φ |



3 Data description

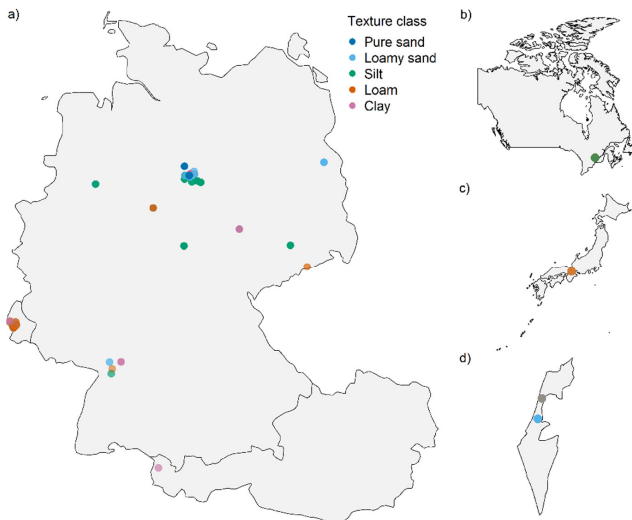
The content of the data collection consists of structured in the following sections: (i) meta data (file: MetaData.csv), (ii) basic soil properties (BasicProp.csv), and (iii) SHP including measured points of the retention curve and hydraulic conductivity curve (RetMeas.csv, CondMeas.csv), (iv) optimized parameter sets for two SHP models (Param.csv) and (v) data series resulting from both SHP models (HydCurves.csv). Each data set is labelled by a unique Sample-ID for easy joining of the different data tables.

3.1 Meta-data

3.1 Metadata

The [meta-data](#) table summarizes relevant information about the availability of the single variables in each data set. All 572 [data-sets](#) contain SHP measurements by the evaporation method, 499 contain at least one dew point measurement and 409 data sets include K_{sat} measurements (Table 2). In 370 data sets all three kinds of SHP information are available. In case of the basic soil properties, soil texture and bulk density are available for all [data-sets](#) and C_{org} is [available](#) in 488 cases. Complete information about all variables (SHP and basic soil properties) is [available](#) in 315 data sets (57 %).

The data collection contains location information for each data set (Figure 1). Most of the samples have been taken in Central Europe ($n = 508$) and only few 555 data sets come from Canada ($n = 29$), Japan ($n = 5$) and Israel ($n = 30$) (see Appendix Figure A1). The sampling sites are not arranged systematically, since as the region of sampling has not been a criterion for data collection. They are rather clustered in the regions where the data-contributing institutions|groups have performed field work. Most of the samples have been taken in Central Europe ($n = 508$). Few data sets come from Canada ($n = 29$), Japan ($n = 5$) and Israel ($n = 30$).



270
271 **Figure 1:** Locations of the sampling sites in (a) Luxembourg, Germany and Austria, (b) Canada, (c) Japan, and (d) Israel. Please+
272 note that the map scales differ, as the maps should only provide a broad overview.

Formatiert: Standard, Abstand Nach: 10 Pt.

Formatiert: Schriftart: 9 Pt., Fett

273
274
275
276 **Table 2: Availability of the key variables contained in the data collection, laboratory method used for analyses and number of+
277 available samples.**

| Measured variable | Number of data sets | |
|--|---------------------|---------------|
| | available | not available |
| SHP by Evaporation method | 572 | 0 |
| SHP by air entry point of tensiometers | 286 | 286 |
| Retention data by dew point method | 499 | 73 |
| Separately measured K_{sat} | 409 | 163 |
| Bulk density | 572 | 0 |
| Texture main groups (SSC) | 572 | 0 |
| Texture subgroups | 569 | 3 |
| C_{org} | 488 | 84 |

Formatiert: Schriftart: 9 Pt., Fett, Schriftfarbe: Schwarz

Formatiert: Standard, Abstand Nach: 10 Pt., Rahmen: Oben: (Kein Rahmen), Unten: (Kein Rahmen), Links: (Kein Rahmen), Rechts: (Kein Rahmen), Zwischen : (Kein Rahmen)

Formatiert: Schriftart: 9 Pt., Fett, Schriftfarbe: Schwarz

Formatiert: Schriftart: 9 Pt., Fett, Schriftfarbe: Schwarz

Formatiert: Schriftart: 9 Pt., Fett

Formatiert: Schriftart: 9 Pt., Fett, Schriftfarbe: Schwarz

Formatiert: Schriftfarbe: Schwarz

Formatiert: Standard, Rahmen: Oben: (Kein Rahmen), Unten: (Kein Rahmen), Links: (Kein Rahmen), Rechts: (Kein Rahmen), Zwischen : (Kein Rahmen), Tabstopps: 7,96 cm, Zentriert + 15,92 cm, Rechtsbündig

| <u>Measured variable</u> | <u>Laboratory method</u> | <u>Number of available samples</u> |
|--|---|------------------------------------|
| <u>Hydraulic Properties of unsaturated soil</u> | <u>Evaporation method (HYPROP)</u> | <u>572</u> |
| | <u>Added measurements by air entry point of tensiometer (Schindler et al., 2010)</u> | <u>286</u> |
| | <u>Added retention measurements by dew point method (Campbell et al., 2007)</u> | <u>499</u> |
| <u>Hydraulic conductivity of saturated soil</u> | <u>Falling head or constant head method</u> | <u>409</u> |
| <u>Bulk density</u> | <u>Weight of oven dried (105°C) undisturbed samples</u> | <u>572</u> |
| <u>Soil texture (63...2000 µm)</u> | <u>Wet sieving with 2000, 630, 200, 63 µm sieves</u> | <u>572</u> |
| <u>Soil texture ($\leq 63 \mu\text{m}$)</u> | <u>Pipette method (Köhn, 1931)</u> | <u>300</u> |
| | <u>Pipette method (Moshrefi, 1993)</u> | <u>78</u> |
| | <u>Hydrometer method</u> | <u>52</u> |
| | <u>Integral suspension pressure method (Durner et al., 2017, Durner and Iden, 2021)</u> | <u>94</u> |
| | <u>Method unknown</u> | <u>48</u> |
| <u>Soil organic carbon content</u> | <u>High-temperature combustion</u> | <u>488</u> |

278

3.2 Basic soil properties

The data collection covers a wide range of soil textures, including soils with up to 65 % clay and 93 % silt and 100 % sand (positions of symbols in the soil texture triangle, Figure 2a and 2b). It covers the textures most frequently found in natural soiltemperate climates. The main textural classes according to the German classification (Ad-hoc-Arbeitsgruppe Boden, 2005) account for 217 (sand), 146 (silt), 422 (loam) and 88 (clay) data sets. (Figure 1a). The sandy soils are further subdivided into 39 samples for pure sand and 178 samples for loamy sand, as the SHP usually have the highest

Formatiert: Schriftart: Fett, Schriftfarbe: Schwarz

Formatiert: Schriftfarbe: Schwarz

Formatiert: Standard, Abstand Vor: 12 Pt., Nach: 12 Pt., Nicht vom nächsten Absatz trennen, Rahmen: Oben: (Kein Rahmen), Unten: (Kein Rahmen), Links: (Kein Rahmen), Rechts: (Kein Rahmen), Zwischen : (Kein Rahmen)

Formatiert: Schriftfarbe: Schwarz

Formatiert: Standard, Rahmen: Oben: (Kein Rahmen), Unten: (Kein Rahmen), Links: (Kein Rahmen), Rechts: (Kein Rahmen), Zwischen : (Kein Rahmen), Tabstopps: 7,96 cm, Zentriert + 15,92 cm, Rechtsbündig

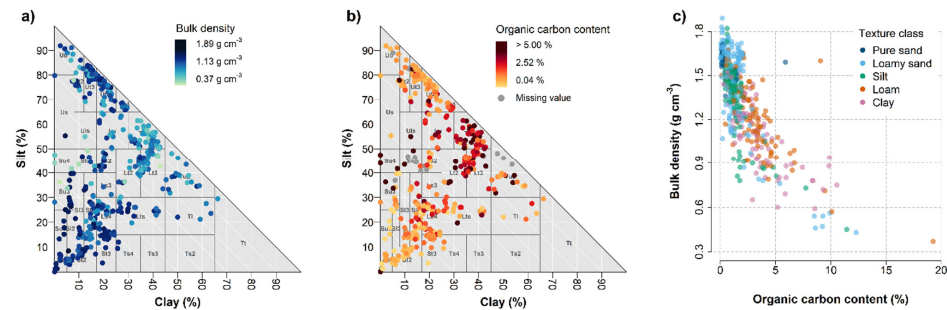
285 variation within the sand texture class. The two areas in the soil texture triangle with the lowest data coverage are sandy clay
 286 and sandy silt soils. Figure 1d shows the colour coded samples in the USDA texture triangle to provide orientation for
 287 international readers.

288 The bulk densities density of the samples varies between 0.37 g cm^{-3} and 1.89 g cm^{-3} with a median of 1.40 g cm^{-3} . High
 289 bulk densities density mainly occurs in sandy soils while silty clay soils were less dense (Figure 2a1b and 1e). In
 290 general, soil bulk density scatters across the texture triangle, which is reflected by rather weak but significant Pearson
 291 correlations ($p\text{-value} < 0.05$) between bulk density and the sand ($r = 0.41$), silt ($r = -0.24$) and clay ($r = -0.50$) contents,
 292 respectively.

293 C_{org} in the samples ranges from 0.04 % to 19.26 % with a median of 1.44 %. The maximum values occur mainly in
 294 silty clay, loam and silty sand soils. Smaller C_{org} values were associated with sand and silt soils (Figure 2b). C_{org} and bulk
 295 density were negatively correlated ($r = -0.76$; Fig. 2e1f).

296 In addition to the standard soil texture classification by sand, silt and clay fractions, the subgroups (coarse, middle, fine) for
 297 silt and sand (i.e. coarse sand, medium sand, fine sand, coarse silt, medium silt, and fine silt) are also provided for the German
 298 classification system (Figure 32a). Most silt soils contain a maximum fraction of coarse silt (20 μm - 63 μm), while the loamy
 299 sands are mainly dominated by the fine sand fraction (63 μm - 200 μm). In contrast to the weak correlation between soil
 300 texture with C_{org} and bulk density, the latter are negatively correlated to each other ($r = -0.76$; Figure 2b).

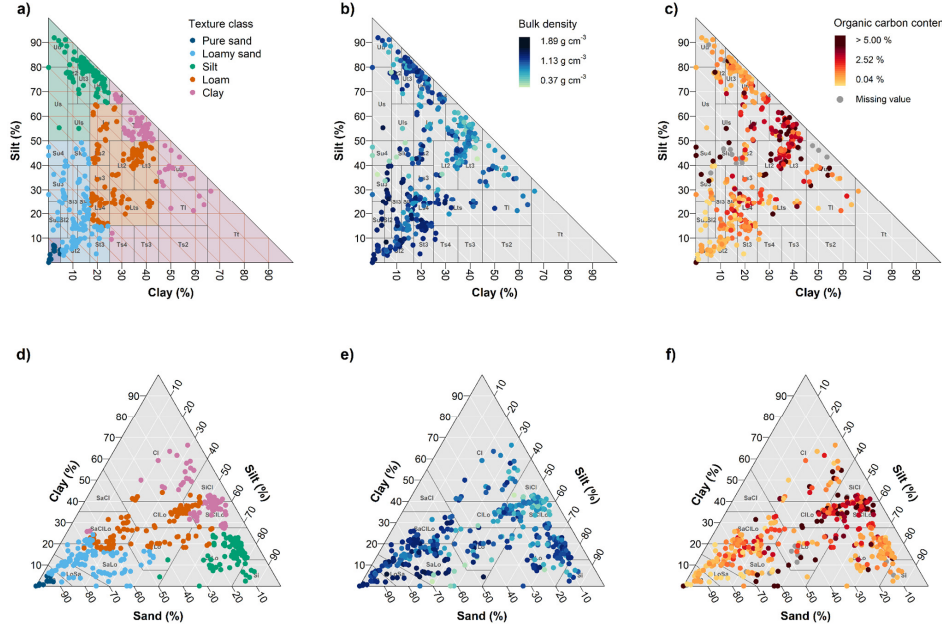
301



302

Formatiert: Schriftfarbe: Schwarz

Formatiert: Standard, Rahmen: Oben: (Kein Rahmen), Unten: (Kein Rahmen), Links: (Kein Rahmen), Rechts: (Kein Rahmen), Zwischen : (Kein Rahmen), Tabstopps: 7,96 cm, Zentriert + 15,92 cm, Rechtsbündig



303
304 **Figure 21:** Distributions of (a, d) texture classes, (b, e) bulk density and (c, f) organic carbon content in the texture triangle of the
305 German (a-c) and (e) the negative correlation between them USDA (d-f) systematic.

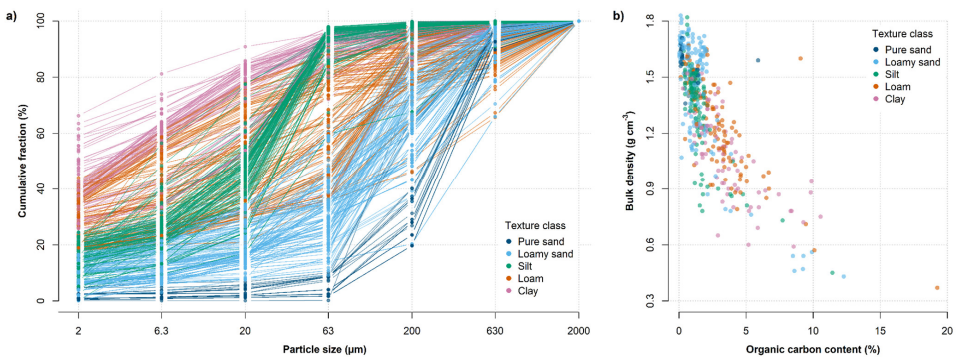
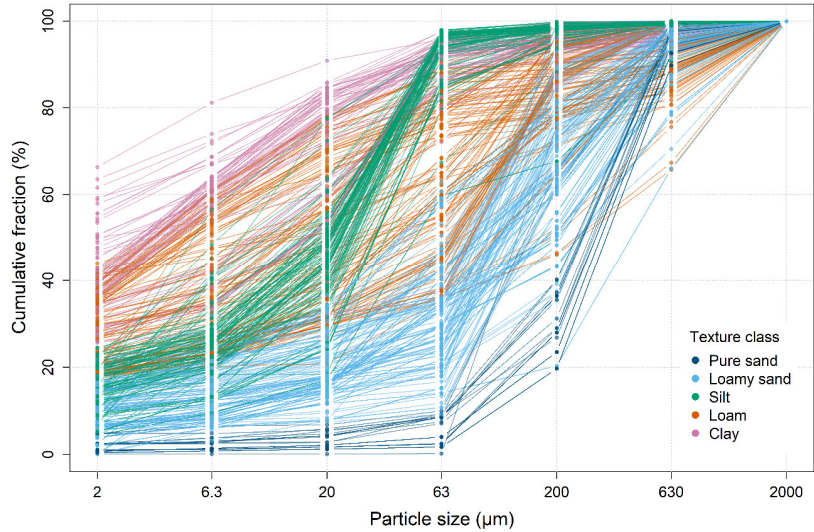
Formatiert: Schriftart: 9 Pt., Fett, Schriftfarbe: Schwarz

Formatiert: Standard, Abstand Nach: 10 Pt., Rahmen: Oben: (Kein Rahmen), Unten: (Kein Rahmen), Links: (Kein Rahmen), Rechts: (Kein Rahmen), Zwischen : (Kein Rahmen), Tabstopps: 7,96 cm, Zentriert + 15,92 cm, Rechtsbündig

Formatiert: Schriftart: 9 Pt., Fett, Schriftfarbe: Schwarz

Formatiert: Schriftfarbe: Schwarz

Formatiert: Standard, Rahmen: Oben: (Kein Rahmen), Unten: (Kein Rahmen), Links: (Kein Rahmen), Rechts: (Kein Rahmen), Zwischen : (Kein Rahmen), Tabstopps: 7,96 cm, Zentriert + 15,92 cm, Rechtsbündig



Formatiert: Schriftfarbe: Schwarz

Formatiert: Standard, Rahmen: Oben: (Kein Rahmen), Unten: (Kein Rahmen), Links: (Kein Rahmen), Rechts: (Kein Rahmen), Zwischen : (Kein Rahmen), Tabstopps: 7,96 cm, Zentriert + 15,92 cm, Rechtsbündig

311 **Figure 3-2:** a) Cumulative particle size distributions of the 572 samples. different textures are distinguished by colour codes. The
312 texture classification refers to the German classification system (Ad hoc Arbeitsgruppe Boden, 2005), but USDA-
313 Scatterplot of C_{org} and bulk density ($r=0.76$). The reference texture classes are also provided in the data collection colour coded.

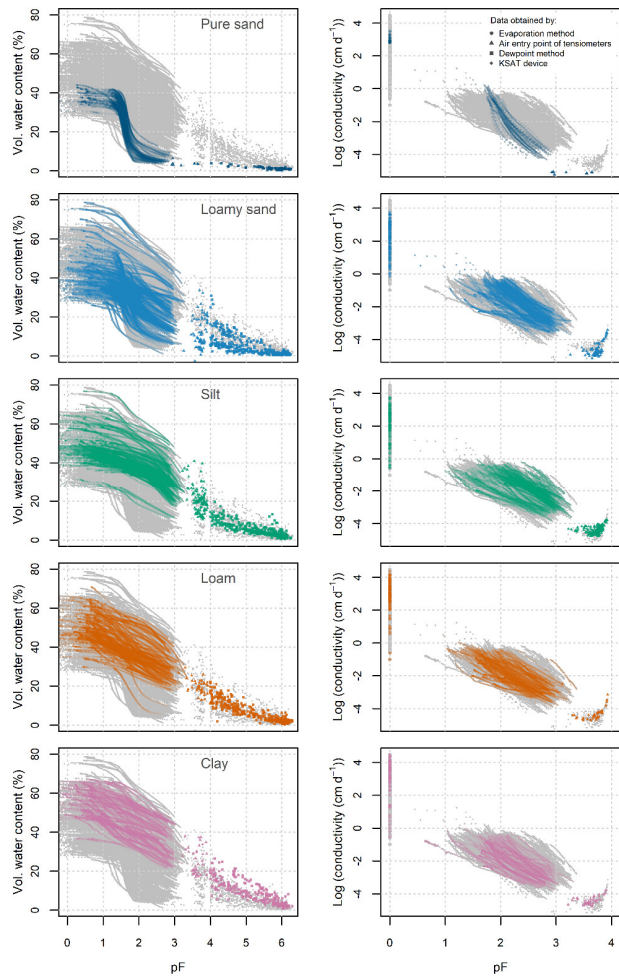
314 3.3 Measured soil hydraulic data

315 The measured SHP are shown in Figure 4. The retention data cover almost the entire range between full water saturation and
316 oven dryness. The highest data coverage is available in the wet and medium saturation range with $pF < 3.2$, where the data
317 stem from the simplified evaporation method (circles in Figure 4). Half of the data sets datasets contain one additional data
318 point between $pF 3.0$ and $pF 4.0$ which originates from the air entry pressure of the porous tensiometers cup (triangles in Figure
319 4). In 499 data sets at least one data pair between $pF 4.0$ and $pF 6.3$ determined by the dewpoint method exists (squares in
320 Figure 4). To cover the drying branch towards $pF 6.8$ the number of dewpoint measurements for single samples ranges
321 between 1 and 8 (with a median of 3), because this method can only assess the matric head values after each reading of the
322 respective sample states.

323 Hydraulic conductivity data obtained by the evaporation method range mostly from $pF 1.0$ to $pF 3.2$. Again, one single
324 conductivity data point originates from the air-entry of the porous cup for about half of the data sets datasets. A separately
325 measured K_{sat} is available for 409 data sets (diamonds in Figure 4) datasets. The data collection neither contains conductivity
326 data in the range close to saturation ($pF < 1$), nor in the dry range. Currently, there is no standard laboratory method to determine
327 hydraulic conductivity in this range. In the online version in Figure 3 the different methods contributing to the retention and
328 conductivity data are plotted as circles (evaporation), triangles (air entry point), squares (dewpoint) and diamonds (K_{sat}). Figure
329 4 presents the same data colour coded by bulk density.

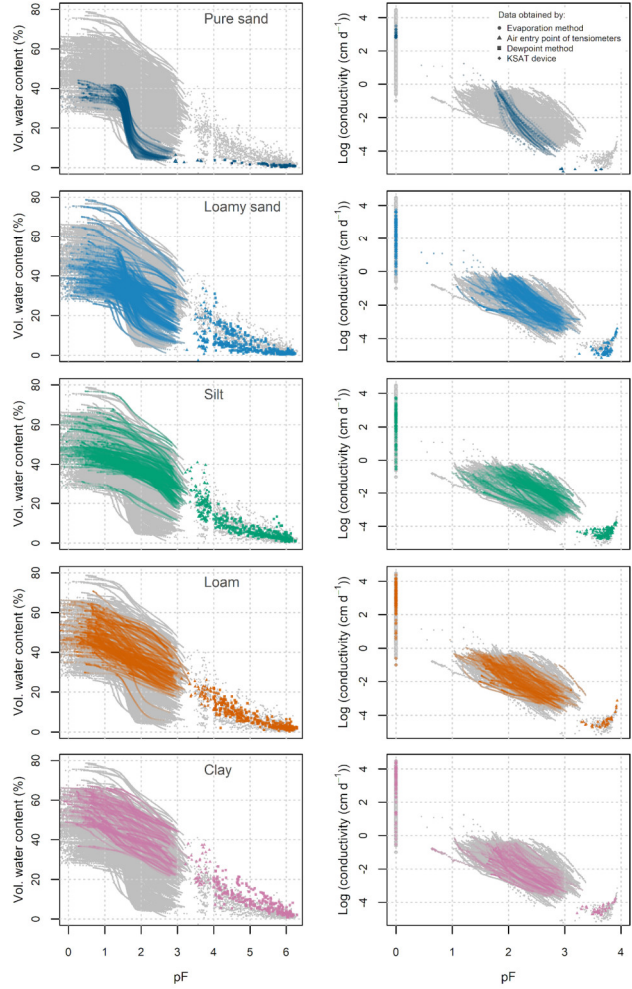
Formatiert: Schriftart: 9 Pt., Fett, Schriftfarbe: Schwarz
Formatiert: Standard, Abstand Nach: 10 Pt., Rahmen: Oben: (Kein Rahmen), Unten: (Kein Rahmen), Links: (Kein Rahmen), Rechts: (Kein Rahmen), Zwischen : (Kein Rahmen)
Formatiert: Schriftart: 9 Pt., Fett, Schriftfarbe: Schwarz
Formatiert: Schriftfarbe: Schwarz
Formatiert: Schriftart: Fett, Schriftfarbe: Schwarz
Formatiert: Schriftfarbe: Schwarz

Formatiert: Schriftfarbe: Schwarz
Formatiert: Standard, Rahmen: Oben: (Kein Rahmen), Unten: (Kein Rahmen), Links: (Kein Rahmen), Rechts: (Kein Rahmen), Zwischen : (Kein Rahmen), Tabstopps: 7,96 cm, Zentriert + 15,92 cm, Rechtsbündig



Formatiert: Schriftfarbe: Schwarz

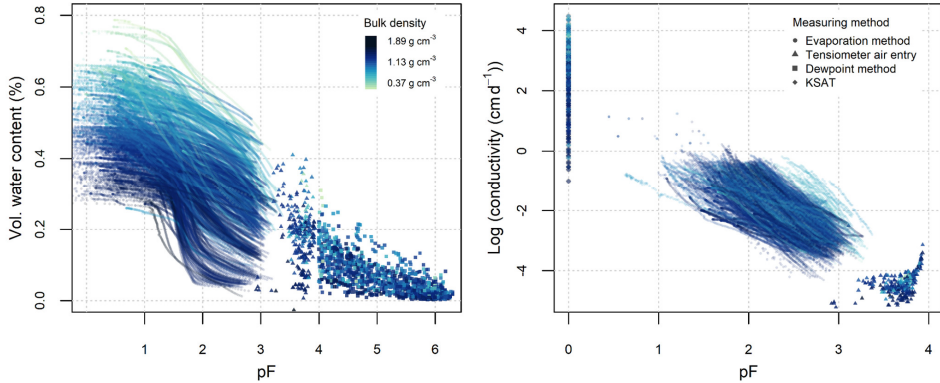
Formatiert: Standard, Rahmen: Oben: (Kein Rahmen), Unten: (Kein Rahmen), Links: (Kein Rahmen), Rechts: (Kein Rahmen), Zwischen : (Kein Rahmen), Tabstopps: 7,96 cm, Zentriert + 15,92 cm, Rechtsbündig



331
332 **Figure 3:** Soil water retention (left) and hydraulic conductivity (right) grouped and colour coded by texture class. Grey background
333 symbols show all measured values. Please note the different pF ranges for the retention and conductivity curves. In the online version
334 the different laboratory methods contributing to the retention and conductivity data are plotted as circles (evaporation), triangles
335 (air entry point), squares (dewpoint) and diamonds (K_{sat}) visible after zooming in.

Formatiert: Schriftfarbe: Schwarz

Formatiert: Standard, Rahmen: Oben: (Kein Rahmen), Unten: (Kein Rahmen), Links: (Kein Rahmen), Rechts: (Kein Rahmen), Zwischen : (Kein Rahmen), Tabstopps: 7,96 cm, Zentriert + 15,92 cm, Rechtsbündig



336
337 **Figure 4:** Soil water retention (left) and hydraulic conductivity (right) measured with different laboratory methods. Grey symbols
338 in the background show all measured values. Data series for single texture classes are summarized in sub plots and indicated
339 by colour codes, colour coded by bulk density. Please note the different pF ranges for the retention and conductivity curves. A more
340 detailed version with the used texture classes is in the Appendix Figure A2. In the online version the different laboratory methods
341 contributing to the retention and conductivity data are plotted as circles (evaporation), triangles (air entry point), squares (dewpoint)
342 and diamonds (K_{sat}) visible after zooming in.

3.4 Fitted SHP models

343 The distributions of the fitted model parameters for both VGM and PDI (data provided in table “Param.csv” in Hohenbrink et
344 al. (2023), but not shown here) mostly cover the predefined range of plausible parameters (Table 1). The constraining
345 boundaries were only hit in 5 cases with the exception of except for parameter λ of the PDI model (154 cases in which bounds
346 were hit).

347 The fitted water retention curves (Figure 5a and 5c) reflect the main characteristics of the measured SHP described above
348 ([Figure 4](#)). Retention curves from both models are similar in the wet to medium range. However, in the medium to dry moisture
349 range they systematically differ. The retention curves described by VGM approach a residual-water content, between 0% and
350 28%, while those from the PDI model linearly consistently reach zero saturation at $pF_{pF} = 6.8$, which reflects the matric
351 potential at oven dryness (Schneider and Goss, 2012). The hydraulic conductivity curves described by VGM (Figure 5b) vary
352 over a wide range. While it is It proves difficult to visually relate them the curves to respective texture visually, those classes,
353 because the wet range part scales strongly with the existence of the larger pores, and the shape of the curve is strongly limited
354 by the underlying linear fit in log-log space. The PDI model curves (Figure 5d) are more closely related to texture and span a
355 much narrower range for each texture class. The variation among the curves decreases towards the dry end of the saturation
356 range. Especially in the dry range, the hydraulic conductivity increases along the texture gradient from pure sand via loamy
357

Formatiert: Schriftart: 9 Pt., Fett, Schriftfarbe: Schwarz

Formatiert: Schriftart: 9 Pt., Fett

Formatiert: Schriftart: 9 Pt., Fett, Schriftfarbe: Schwarz

Formatiert: Schriftart: 9 Pt., Fett, Schriftfarbe: Schwarz

Formatiert: Standard, Abstand Nach: 10 Pt.

Formatiert: Schriftart: Fett, Schriftfarbe: Schwarz

Formatiert: Standard, Abstand Vor: 12 Pt., Nach: 12 Pt.,
Nicht vom nächsten Absatz trennen, Rahmen: Oben: (Kein Rahmen), Unten: (Kein Rahmen), Links: (Kein Rahmen), Rechts: (Kein Rahmen), Zwischen : (Kein Rahmen)

Formatiert: Schriftfarbe: Schwarz

Formatiert: Schriftfarbe: Schwarz

Formatiert: Standard, Rahmen: Oben: (Kein Rahmen),
Unten: (Kein Rahmen), Links: (Kein Rahmen), Rechts: (Kein Rahmen), Zwischen : (Kein Rahmen), Tabstopps: 7,96 cm,
Zentriert + 15,92 cm, Rechtsbündig

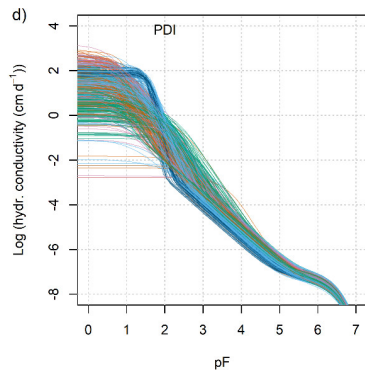
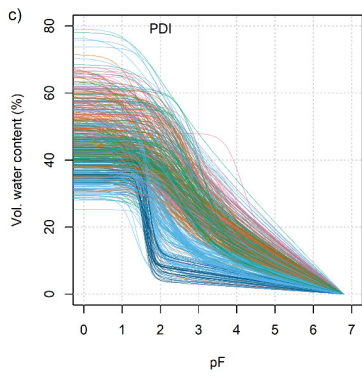
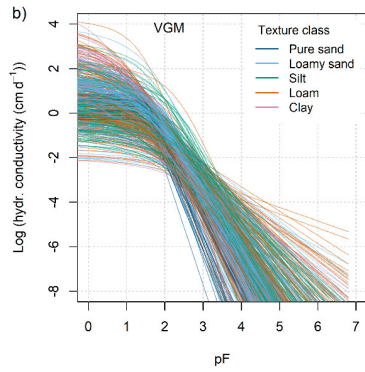
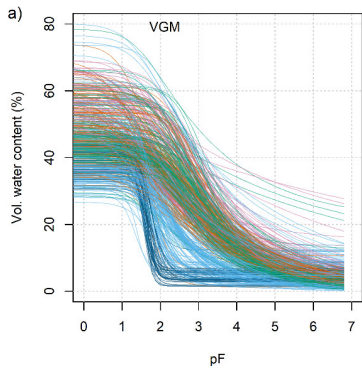
359 sand, silt and loam to clay. This phenomenon results from the PDI model structure, where hydraulic conductivity in the dry
360 range is directly derived from the water content at $pF_{pF} = 5.0$ (Peters et al., 2021). At pF (Peters et al., 2021). At $pF > 5.5$
361 the hydraulic conductivity of the PDI model is dominated by the isothermal vapour conductivity for all textures texture classes.
362 Common As an estimate for soil hydrological key properties to evaluate the ability of a soil to support plant growth can be water
363 characteristics, we derived from the fitted water retention curves : the soil water content at field capacity (θ at $pF_{pF} = 1.8$)
364 and), soil water content at the permanent wilting point (θ at $pF_{pF} = 4.2$), as well as the resulting plant available water content
365 ($\theta(pF = 1.8) - \theta(pF = pF 4.2)$). Figure 6 shows these values in the texture triangle derived from calculated based
366 on the PDI retention curves. The water content at both, field capacity (Figure 6a) and wilting point (Figure 6b), roughly
367 increases from sandy soils towards soils with finer textures. However, apart from this very general distinction, the values of
368 both variables vary widely over the texture triangle. The same pattern applies to, which directly results from the values variation
369 of plant the retention curves within a single texture class (Figure 5c). Plant available water content, which (Figure 6c) depicts
370 the same high variability within the texture triangle. It varies between the extremes of 3.8 % (v/v) vol. % in pure sand up to
371 49.2 % (v/v) vol. % in the fine-textured soils—soil but does not align to any clear, texture-related pattern.

372
373

Formatiert: Schriftart: (Intl) Cambria Math

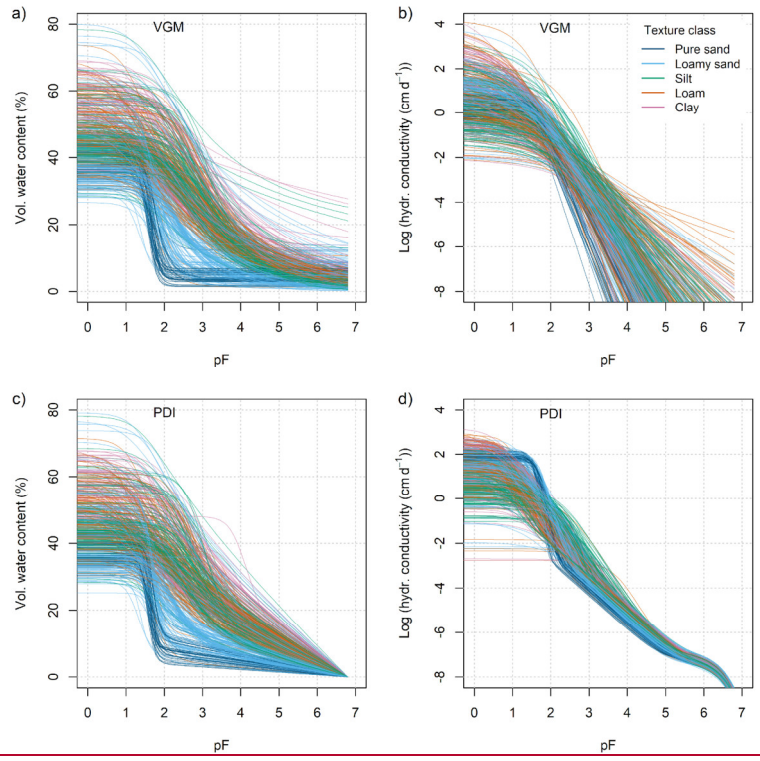
Formatiert: Schriftfarbe: Schwarz

Formatiert: Standard, Rahmen: Oben: (Kein Rahmen), Unten: (Kein Rahmen), Links: (Kein Rahmen), Rechts: (Kein Rahmen), Zwischen : (Kein Rahmen), Tabstopps: 7,96 cm, Zentriert + 15,92 cm, Rechtsbündig



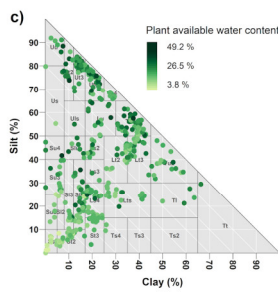
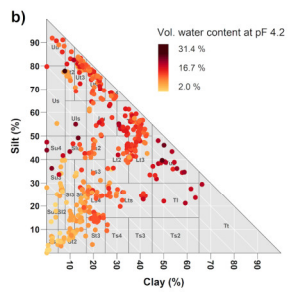
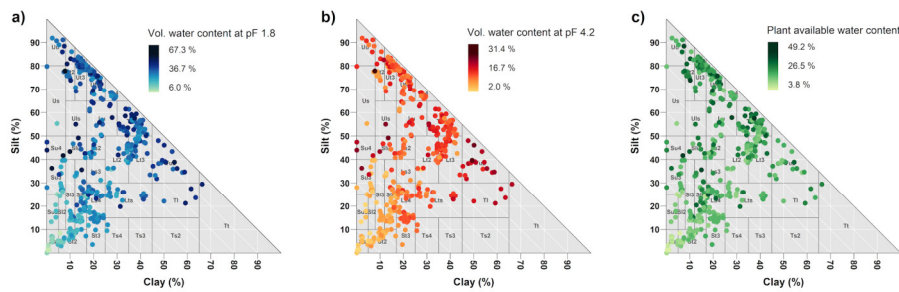
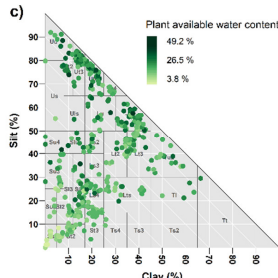
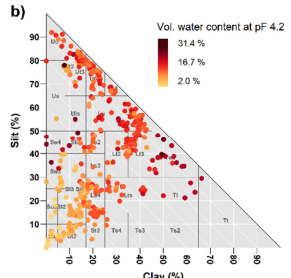
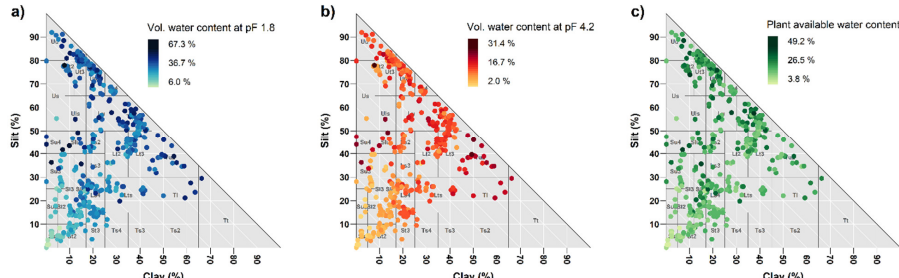
Formatiert: Schriftfarbe: Schwarz

Formatiert: Standard, Rahmen: Oben: (Kein Rahmen), Unten: (Kein Rahmen), Links: (Kein Rahmen), Rechts: (Kein Rahmen), Zwischen : (Kein Rahmen), Tabstopps: 7,96 cm, Zentriert + 15,92 cm, Rechtsbündig



375
376 **Figure 5:** Retention curves (left, a and c) and hydraulic conductivity curves (right, b and d) for the van Genuchten-Mualem model (a and b) and the PDI model with van Genuchten-VGM basic function (c and d). Soil texture classes are indicated by different
377 colour codes.
378

- 379 **Formatiert:** Schriftart: 9 Pt., Fett, Schriftfarbe: Schwarz
- Formatiert:** Schriftart: 9 Pt., Fett
- Formatiert:** Standard, Abstand Nach: 10 Pt., Rahmen: Oben: (Kein Rahmen), Unten: (Kein Rahmen), Links: (Kein Rahmen), Rechts: (Kein Rahmen), Zwischen : (Kein Rahmen)
- Formatiert:** Schriftart: 9 Pt., Fett, Schriftfarbe: Schwarz
- Formatiert:** Schriftfarbe: Schwarz
- Formatiert:** Schriftfarbe: Schwarz
- Formatiert:** Standard, Rahmen: Oben: (Kein Rahmen), Unten: (Kein Rahmen), Links: (Kein Rahmen), Rechts: (Kein Rahmen), Zwischen : (Kein Rahmen), Tabstopps: 7,96 cm, Zentriert + 15,92 cm, Rechtsbündig



382 **Figure 6.** Volumetric water contents at (a) field capacity, (b) the plant wilting point and (c) the resulting plant available water scattered on the soil texture triangle. The values provided in the data collection are calculated from retention curves described by
383 the PDI model.

385 **4 Discussion**

386 **4.1 New applications arising from the data collection**

387 The combination of different state-of-the-art methods to measure soil water retention and hydraulic conductivity based on
388 undisturbed samples yields a unique SHP data collection. Especially, the denser coverage of a wider range of saturation levels
389 compared to existing data collections makes this one valuable for new applications. For example, the retention data in the
390 dry range measured with the dewpoint method represent essential information to develop retention models that overcome the
391 concept of a residual water content, which has been shown to be not physically consistent (e.g. Schneider and Goss, 2012;
392 Tuller and Or, 2005; Nimmo, 1991). Furthermore, this data collection provides measurements of both saturated and unsaturated
393 hydraulic conductivity for each of the 572 samples in high resolution and over a wide range of saturation levels. This supports
394 the development and improvement of hydraulic conductivity models.

Formatiert: Schriftart: 9 Pt., Fett, Schriftfarbe: Schwarz

Formatiert: Standard, Abstand Nach: 10 Pt., Rahmen: Oben: (Kein Rahmen), Unten: (Kein Rahmen), Links: (Kein Rahmen), Rechts: (Kein Rahmen), Zwischen : (Kein Rahmen)

Formatiert: Schriftart: 9 Pt., Fett

Formatiert: Schriftart: 9 Pt., Fett, Schriftfarbe: Schwarz

Formatiert: Schriftart: 9 Pt., Fett, Schriftfarbe: Schwarz

Formatiert: Schriftfarbe: Schwarz

Formatiert: Schriftart: Fett, Schriftfarbe: Schwarz

Formatiert: Schriftart: Fett, Schriftfarbe: Schwarz

Formatiert: Schriftfarbe: Schwarz

Formatiert: Schriftfarbe: Schwarz

Formatiert: Standard, Rahmen: Oben: (Kein Rahmen), Unten: (Kein Rahmen), Links: (Kein Rahmen), Rechts: (Kein Rahmen), Zwischen : (Kein Rahmen), Tabstopps: 7,96 cm, Zentriert + 15,92 cm, Rechtsbündig

395 An additional advantage of this data collection is that it is based on undisturbed samples exhibiting features of natural soils.
396 Thereby it can be tested whether SHP models are suitable to describe the SHP for more practical applications. When an SHP
397 model is only developed and tested with packed soil columns or with samples from few carefully selected sites, it might behave
398 less robust in “real world” applications.

399 The high level of standardisation using the described methods enables us to link data from various labs without methodological
400 offsets commonly found due to slightly deviating soil sample processing. Although the data set does not reach any global
401 coverage, the data set exceeds existing SHP data collections by data density, extent of the values and variables, and consistency.
402 We envision the proposed data structure as a foundation for upcoming additions with the methods becoming more and more
403 accessible.

404 The VGM and PDI parameters provided in the data collection have been estimated with state-of-the-art techniques. Both
405 parameter sets can be valuable to develop and test simulation models and to perform simulation studies. They can also serve
406 as a benchmark for further developments of non-linear parameter estimation algorithms. We have intentionally omitted the
407 measured K_{sat} values during parameter estimation. Considering K_{sat} in combination with unimodal SHP models usually causes
408 an overestimation of hydraulic conductivity close to saturation since the K_{sat} information mainly reflects the impact of soil
409 structure (Durner, 1994; Peters et al., 2023). The K_s parameter derived for the PDI can thus be interpreted as the conductivity
410 of the soil matrix only, excluding effects of soil structure similarly to Weynants et al. (2009), and as further discussed in
411 Fatichi et al. (2020). It is now possible to further investigate the relation between K_s of the soil matrix and K_{sat} of the entire soil
412 including structure effects based on the parameters provided.

413 Besides In addition to the commonly used three fractions of sand, silt and clay to classify soil texture, they provide subgroups
414 for sand and silt are also provided in the data collection. The effect of the resolution of particle size classification on SHP has
415 rarely been investigated, and common. Most pedotransfer functions only consider the three main texture groups as predictor
416 variables. However, SHPs are expected to differ significantly when the sand fraction is dominated by either fine sand or coarse
417 sand. Based on the presented data collection, such questions can be investigated Our data suggests that the main texture classes
418 alone contain limited information about soil hydrologic properties (large spread of hydraulic curves within texture classes in
419 Figure 3, scattered texture distribution for plant available water in detail and potentially Figure 6c). Only in combination with
420 bulk density and C_{org} , the data becomes more accurate informative (Figure 4 and A2). For advancing pedotransfer functions
421 can be developed, the presented data collection is a promising basis for analyses of (i) the resolution of texture data and texture
422 class delineation (c.f. Twarakavi et al., 2010), (ii) the resolution of the SHP data series and (iii) suitable indicators for
423 hydrologic functioning (field capacity, wilting point, etc. c.f. Assouline and Or, 2014).

424 4.2 Limitations of the data collection and further research needs

425 Although the data collection enables many different applications, it has some limitations that must be considered when
426 analysing the data and interpreting the results. The single data sets are not completely statistically independent from each other

Formatiert: Schriftfarbe: Schwarz

Formatiert: Schriftfarbe: Schwarz

Formatiert: Schriftfarbe: Schwarz, Englisch (Vereinigtes Königreich)

Formatiert: Schriftfarbe: Schwarz

Formatiert: Schriftfarbe: Schwarz

Formatiert: Schriftfarbe: Schwarz

Formatiert: Schriftfarbe: Schwarz

Formatiert: Schriftfarbe: Benutzerdefinierte Farbe(RGB(153;0;255))

Formatiert: Schriftart: Fett, Schriftfarbe: Schwarz

Formatiert: Standard, Abstand Vor: 12 Pt, Nach: 12 Pt, Mit Gliederung + Ebene: 2 + Nummerierungsformatvorlage: 1, 2, 3, ... + Beginnen bei: 1 + Ausrichtung: Links + Ausgerichtet an: 0 cm + Einzug bei: 0,63 cm, Nicht vom nächsten Absatz trennen, Rahmen: Oben: (Kein Rahmen), Unten: (Kein Rahmen), Links: (Kein Rahmen), Rechts: (Kein Rahmen), Zwischen : (Kein Rahmen)

Formatiert: Schriftfarbe: Schwarz

Formatiert: Schriftfarbe: Schwarz

Formatiert: Standard, Rahmen: Oben: (Kein Rahmen), Unten: (Kein Rahmen), Links: (Kein Rahmen), Rechts: (Kein Rahmen), Zwischen : (Kein Rahmen), Tabstopps: 7,96 cm, Zentriert + 15,92 cm, Rechtsbündig

427 for the following main reasons: (i) many samples stem from identical sites; (ii) some data sets exhibit identical texture and C_{org}
428 values, because in somethese cases only few aggregated disturbed samples representative for a whole site have been taken;
429 (iii) the analyses have been performed in five different laboratories. However, by closely following the guidelines of the
430 experiments a high degree of standardisation in the laboratory protocols could be achieved.

431 In some situations, it might be reasonable to thin out the data by keeping only data sets assumed to be statistically independent.
432 However, whether this is necessary depends on the particular research question and the applied data analysing technique. We
433 have decided to include all available data sets, and to provide enough meta information to evaluate the statistical dependencies,
434 and leave it up to the user to decide how to handle #such dependencies.

435 Another feature|limitation of the data that users have to must cope with is the unbalanced distribution of the datasets in terms
436 of basic soil properties. For example, Luvisols with silt contents between 70 % and 85 % are overrepresented in the data
437 collection due to their agricultural importance which leadsled to more frequent soil analyses. In contrast, there are data gaps
438 for the sandy clay and sandy silt texture classes, because they do occur more sparsely in naturethe regions under study and are
439 generally less intensively investigated. The unbalanced distribution of the data can be especially challenging for the
440 development of pedotransfer functions. This problem can be best solved by supplementing the data collection by additional
441 measurements, but this is a major task at the level of the soil hydrological community and can hardly be achieved by individual
442 researchers.

443 At the level of individual datasets, the gaps in the hydraulic conductivity series near saturation and under dry conditions are
444 another important limitation. Such data are needed to parameterize existing models in a way that they become more reliable
445 in the respective saturation ranges. More comprehensive hydraulic conductivity data is also required to develop new SHP
446 models. Therefore, we identify a need for developing and establishing new standard methods to measure hydraulic conductivity
447 close to saturation (Sarkar et al., 2019b, a) and in the dry range.

Formatiert: Schriftfarbe: Schwarz
Formatiert: Schriftfarbe: Automatisch
Formatiert: Schriftfarbe: Automatisch

Formatiert: Schriftfarbe: Automatisch
Formatiert: Schriftfarbe: Schwarz

Formatiert: Schriftfarbe: Automatisch

448 4.3 Implications for lab procedures and further extension of the data collection

449 The different texture class definitions required us to estimate the missing breakpoint between USDA sand and silt fractions
450 based on monotone cubic splines fitted to the German cumulative particle size distributions as recommended by Nemes et al.
451 (1999). While this technique appears perfectly feasible given the high level of detail in the texture data with seven classes, this
452 would have been more uncertain when the data would have been limited to the three main texture classes. The estimate can be
453 eliminated altogether, when the 63 μm sieve and the 50 μm sieve are included as standard.

454 Despite the high level of standardisation using the described techniques to determine SHPs, the quality check based on the
455 procedure presented in section 2.4 proved to be important to avoid erroneous interpretations and to ensure data quality. When
456 followed, data from different labs can be easily combined. It would be favourable if this could be extended to further relevant
457 soil properties e.g. soil texture, C_{org} , Mid-Infrared reflection spectra. We encourage the community to use and extend this data
458 collection.

Formatiert: Schriftfarbe: Schwarz
Formatiert: Standard, Rahmen: Oben: (Kein Rahmen),
Unten: (Kein Rahmen), Links: (Kein Rahmen), Rechts: (Kein Rahmen), Zwischen : (Kein Rahmen), Tabstopps: 7,96 cm,
Zentriert + 15,92 cm, Rechtsbündig

459 5 Data availability

460 The data collection is hosted in the repository GFZ Data Services (Hohenbrink et al, 2023). It can be accessed via
461 <https://doi.org/10.5880/fidgeo.2023.012>. The final DOI will be registered when the
462 paper is accepted, temporary data access to Hohenbrink et al. (2023) via <https://dataservices.gfz-potsdam.de/panmetaworks/review/5e617ed2664ea4d03e81301b5be2236f0e9620ea0bed66e726d2e424d166fd85/>.
463 The rights of use are defined by a creative common licence (CC BY 4.0). The data collection in the repository includes all data presented
464 in this paper. Further information and materials such as small volumes of air-dried reserve soil samples can be provided by
465 the corresponding author or the second author (Conrad.Jackisch@tbt.tu-freiberg.de) upon request.

469 6 Summary and conclusions

470 Motivated by a need for detailed soil water retention and hydraulic conductivity data, we have launched collected data from
471 572 undisturbed ring samples in a community initiative to collect data. High level of SHP measured using state of the art standardisation in new measurement techniques. After and rigorous quality filtering, our data collection contained allowed
472 for consistency, which is rarely achieved in soil water retention and hydraulic conductivity data sets determined analyses from
473 different labs.
474 Initial comparisons of hydraulic indicators (e.g. plant available water content) with the simplified evaporation method, the
475 dewpoint method and separate K_{sat} measurements for 572 undisturbed soil samples classical texture data showed very weak
476 predictive power by texture. The data sets are supplemented with basic soil properties including addition of more texture classes
477 from the particle size distribution obtained by sieving and sedimentation analyses, as well as and the addition of supplementary
478 data on bulk density and organic carbon contents. In addition to the experimental data, we provide parameter sets and tabulated
479 water retention and conductivity curves over the whole moisture range for two models of SHP: the well-established van
480 Genuchten Mualem model, and the recent version of the PDI model. content appear to be more informative predictors.

481 The data collection can be used in its current form or integrated into existing data collections. All data sets were acquired
482 directly from the original sources, which makes the data collection completely independent of the existing pool of data on SHP
483 and thus contributes to their diversification. In particular, the hydraulic conductivity series will substantially expand the
484 existing inventory of SHP data.

485 We expect that this data collection can serve as an independent, new and therefore unexplored benchmark reference to evaluate
486 already existing SHP models and pedotransfer functions. Due to the high resolution of measured data compared to most data
487 in existing databases and the extended range of saturation, it is also an ideal basis to develop and test new advanced SHP

Formatiert: Schriftart: Fett, Schriftfarbe: Schwarz

Formatiert: Standard, Abstand Vor: 24 Pt., Nach: 12 Pt.,
Nicht vom nächsten Absatz trennen, Rahmen: Oben: (Kein Rahmen), Unten: (Kein Rahmen), Links: (Kein Rahmen), Rechts: (Kein Rahmen), Zwischen : (Kein Rahmen)

Formatiert: Absatz-Standardschriftart

Formatiert: Schriftart: Fett, Schriftfarbe: Schwarz

Formatiert: Standard, Abstand Vor: 24 Pt., Nach: 12 Pt.,
Nicht vom nächsten Absatz trennen, Rahmen: Oben: (Kein Rahmen), Unten: (Kein Rahmen), Links: (Kein Rahmen), Rechts: (Kein Rahmen), Zwischen : (Kein Rahmen)

Formatiert: Englisch (Vereinigtes Königreich)

Formatiert: Englisch (Vereinigtes Königreich)

Formatiert: Englisch (Vereinigtes Königreich)

Formatiert: Englisch (Vereinigtes Königreich)

Formatiert: Schriftfarbe: Automatisch, Englisch (Vereinigtes Königreich)

Formatiert: Schriftfarbe: Automatisch, Englisch (Vereinigtes Königreich)

Formatiert: Englisch (Vereinigtes Königreich)

Formatiert: Englisch (Vereinigtes Königreich)

Formatiert: Englisch (Vereinigtes Königreich)

Formatiert: Schriftfarbe: Schwarz

Formatiert: Standard, Rahmen: Oben: (Kein Rahmen),
Unten: (Kein Rahmen), Links: (Kein Rahmen), Rechts: (Kein Rahmen), Zwischen : (Kein Rahmen), Tabstopps: 7,96 cm,
Zentriert + 15,92 cm, Rechtsbündig

489 models and pedotransfer functions. It is ~~also~~ well suited to verify findings and conclusions that have so far emerged from the
490 existing data collections.

491 **Author contributions**

492 TH compiled and analysed the data, created the figures, and drafted the manuscript, in close collaboration with CJ. All co-
493 authors contributed to the final version. AP adapted the PDI model and the fitting software, was involved in building the data
494 collection, and supervised the project. CJ supported in structuring the data collection. JM, JK, FL, and CJ provided already
495 existing data sets and evaluated them initially. KG and MN collected samples with new combinations of basic soil properties,
496 performed laboratory measurements, and evaluated them initially. AP adapted the PDI model and the fitting software, was
497 involved in building the data collection, and supervised the project. WD and SI supported the data preparation and analyses.

498

499 **Competing Interests**

500 Conrad Jackisch is a member of the editorial board of Earth System Science Data. The authors have ~~also~~ no other competing
501 interests to declare.

502 **Acknowledgements**

503 The initiative of this data collection has emerged from a project funded by the Deutsche Forschungsgemeinschaft (DFG,
504 German Research Foundation grant PE 1912/4-1). TH and MN were funded by the same project. JM was funded by the
505 Collaborative Research Centre AquaDiva of the Deutsche Forschungsgemeinschaft (DFG, German Research Foundation)—
506 SFB 1076—Project Number 218627073. “AquaDiva”, funded as DFG SFB 1076, project number 218627073. CJ and TH were
507 part of the DFG research unit “From Catchments as Organised Systems to Models Based on Functional Units” (FOR 1598)
508 funded as DFG grant ZE 533/9-1. We thank Birgit Walter and Ines Andrae for laboratory analyses of the soil samples taken
509 especially for this initiative. All authors thankfully acknowledge their respective field and lab support. Without their meticulous
510 work this data set would not have come into existence.

511 **References**

512 Ad-hoc-Arbeitsgruppe Boden: Bodenkundliche Kartieranleitung: mit 41 Abbildungen, 103 Tabellen und 31 Listen, edited by:
513 Eckelmann, W., In Kommission: E. Schweizerbart'sche Verlagsbuchhandlung (Nägele und Obermiller), Stuttgart, 2005.

514 Assouline, S. and Or, D.: Conceptual and Parametric Representation of Soil Hydraulic Properties: A Review, VADOSE ZONE
515 J, 12, [httSps://doi.org/10.2136/vzj2013.07.0121](https://doi.org/10.2136/vzj2013.07.0121), 2013.

516 Assouline, S. and Or, D.: The concept of field capacity revisited: Defining intrinsic static and dynamic criteria for soil internal
517 drainage dynamics, Water Resources Research, 50, 4787–4802, <https://doi.org/10.1002/2014wr015475>, 2014.

518 Brooks, R. H. and Corey, A. T.: Hydraulic properties of porous media, Colorado State University, Fort Collins, Colorado,
519 1964.

Formatiert: Schriftart: Fett, Schriftfarbe: Schwarz

Formatiert: Standard, Abstand Vor: 24 Pt., Nach: 12 Pt.,
Nicht vom nächsten Absatz trennen, Rahmen: Oben: (Kein Rahmen), Unten: (Kein Rahmen), Links: (Kein Rahmen),
Rechts: (Kein Rahmen), Zwischen : (Kein Rahmen)

Formatiert: Englisch (Vereinigtes Königreich)

Formatiert

Formatiert: Englisch (Vereinigtes Königreich)

Formatiert: Schriftart: Fett, Schriftfarbe: Schwarz

Formatiert: Standard, Abstand Vor: 24 Pt., Nach: 12 Pt.,
Nicht vom nächsten Absatz trennen, Rahmen: Oben: (Kein Rahmen), Unten: (Kein Rahmen), Links: (Kein Rahmen),
Rechts: (Kein Rahmen), Zwischen : (Kein Rahmen)

Formatiert: Abstand Nach: 12 Pt.

Formatiert: Schriftart: Nicht Fett

Formatiert: Schriftart: Fett, Schriftfarbe: Schwarz

Formatiert: Standard, Abstand Vor: 24 Pt., Nach: 12 Pt.,
Nicht vom nächsten Absatz trennen, Rahmen: Oben: (Kein Rahmen), Unten: (Kein Rahmen), Links: (Kein Rahmen),
Rechts: (Kein Rahmen), Zwischen : (Kein Rahmen)

Formatiert: Schriftfarbe: Schwarz

Formatiert: Standard, Rahmen: Oben: (Kein Rahmen),
Unten: (Kein Rahmen), Links: (Kein Rahmen), Rechts: (Kein Rahmen), Zwischen : (Kein Rahmen), Tabstopps: 7,96 cm,
Zentriert + 15,92 cm, Rechtsbündig

- 520 Campbell, G. S., Smith, D. M., and Teare, B. L.: Application of a Dew Point Method to Obtain the Soil Water Characteristic,
521 in: Experimental unsaturated soil mechanics, Springer, 71–77, https://doi.org/10.1007/3-540-69873-6_7, 2007.
- 522 Carsel, R. F. and Parrish, R. S.: Developing joint probability distributions of soil water retention characteristics, WATER
523 RESOUR RES, 24, 755–769, <https://doi.org/10.1029/WR024i005p00755>, 1988.
- 524 [Duan, Q., Sorooshian, S., and Gupta, V.: Effective and efficient global optimization for conceptual rainfall-runoff models.](#)
525 [WATER RESOUR RES, 28, 1015–1031, https://doi.org/10.1029/91WR02985, 1992.](#)
- 526 Durner, W.: Hydraulic conductivity estimation for soils with heterogeneous pore structure, WATER RESOUR RES, 30, 211–
527 223, <https://doi.org/10.1029/93WR02676>, 1994.
- 528 [Durner, W., Iden, S.C.: The improved integral suspension pressure method \(ISP+\) for precise particle size analysis of soil and](#)
529 [sedimentary materials, SOIL TILL RES, 213, 105086, https://doi.org/10.1016/j.still.2021.105086, 2021.](#)
- 530 [Durner, W., Iden, S.C., von Unold, G.: The integral suspension pressure method \(ISP\) for precise particle-size analysis by](#)
531 [gravitational sedimentation, WATER RESOUR RES, 53, 33–48, https://doi.org/10.1002/2016WR019830, 2017.](#)
- 532 Fatichi, S., Or, D., Walko, R., Vereecken, H., Young, M. H., Ghezzehei, T. A., Hengl, T., Kollet, S., Agam, N., and Avissar,
533 R.: Soil structure is an important omission in Earth System Models, NAT COMMUN, 11, 1–11,
534 <https://doi.org/10.1038/s41467-020-14411-z>, 2020.
- 535 Van Genuchten, M. T.: A Closed-form Equation for Predicting the Hydraulic Conductivity of Unsaturated Soils, SOIL SCI
536 SOC AM J, 44, 892–898, <https://doi.org/10.2136/sssaj1980.03615995004400050002x>, 1980.
- 537 Germer, K. and Braun, J.: Multi-step outflow and evaporation experiments—Gaining large undisturbed samples and comparison
538 of the two methods, J HYDROL, 577, 123914, <https://doi.org/10.1016/j.jhydrol.2019.123914>, 2019.
- 539 Gupta, S., Papritz, A., Lehmann, P., Hengl, T., Bonetti, S., and Or, D.: Global Soil Hydraulic Properties dataset based on
540 legacy site observations and robust parameterization, Scientific Data, 9, 1–15, <https://doi.org/10.1038/s41597-022-01481-5>,
541 2022.
- 542 Iden, S. C., Peters, A., and Durner, W.: Improving prediction of hydraulic conductivity by constraining capillary bundle models
543 to a maximum pore size, ADV WATER RESOUR, 85, 86–92, <https://doi.org/10.1016/j.advwatres.2015.09.005>, 2015.
- 544 Hohenbrink, T. L., Jackisch, C., Durner, W., Germer, K., Iden, S. C., Kreiselmeier, J., Leuther, F., Metzger, J. C., Naseri, M.,
545 Peters, A.: Soil hydraulic characteristics in a wide range of saturation and soil properties. GFZ Data Services.
546 <https://doi.org/10.5880/fidgeo.2023.012>, 2023. DOI registration when the paper is accepted, temporary data access via
547 [https://dataservices.gfz-](https://dataservices.gfz-potsdam.de/pammetworks/review/5c617cd2664ea4d03e81301b5bc2236f0c9620ca0bed66c726d2e424d166fd85/)
548 [potsdam.de/pammetworks/review/5c617cd2664ea4d03e81301b5bc2236f0c9620ca0bed66c726d2e424d166fd85/](https://pammetworks/review/5c617cd2664ea4d03e81301b5bc2236f0c9620ca0bed66c726d2e424d166fd85/).
- 549 Jackisch, C., Angermann, L., Allroggen, N., Sprenger, M., Blume, T., Tronicke, J., and Zehe, E.: Form and function in hillslope
550 hydrology: in situ imaging and characterization of flow-relevant structures, HYDROL EARTH SYST SC,
551 <https://doi.org/10.5194/hess-21-3749-2017>, 2017.
- 552 Jackisch, C., Germer, K., Graeff, T., Andrä, I., Schulz, K., Schiedung, M., Haller-Jans, J., Schneider, J., Jaquemotte, J., Helmer,
553 P., and others: Soil moisture and matric potential—an open field comparison of sensor systems, EARTH SYST SCI DATA, 12,
554 683–697, <https://doi.org/10.5194/essd-12-683-2020>, 2020.

Formatiert: Schriftfarbe: Schwarz

Formatiert: Standard, Rahmen: Oben: (Kein Rahmen), Unten: (Kein Rahmen), Links: (Kein Rahmen), Rechts: (Kein Rahmen), Zwischen : (Kein Rahmen), Tabstopps: 7,96 cm, Zentriert + 15,92 cm, Rechtsbündig

555 Jarvis, N. J.: A review of non-equilibrium water flow and solute transport in soil macropores: principles, controlling factors
556 and consequences for water quality, SOIL SCI., 58, 523-546, <https://doi.org/10.1111/j.1365-2389.2007.00915.x>, 2007.

557 Kirste, B., Iden, S. C., and Durner, W.: Determination of the Soil Water Retention Curve around the Wilting Point: Optimized
558 Protocol for the Dewpoint Method, SOIL SCI SOC AM J, 83, 288–299, <https://doi.org/10.2136/sssaj2018.08.0286>, 2019.

559 Köhn, M.: Die mechanische Analyse des Bodens mittels Pipettmethode. Z PFLANZ BODENKUNDE, 21 (2), 211–222,
560 <https://doi.org/10.1002/jpln.19310210206>, 1931.

561 Kreiselmeier, J., Chandrasekhar, P., Weninger, T., Schwen, A., Julich, S., Feger, K.-H., and Schwärzel, K.: Quantification of
562 soil pore dynamics during a winter wheat cropping cycle under different tillage regimes, SOIL TILL RES, 192, 222–232,
563 <https://doi.org/10.1016/j.still.2019.05.014>, 2019.

Formatiert: Deutsch (Deutschland)

564 Kreiselmeier, J., Chandrasekhar, P., Weninger, T., Schwen, A., Julich, S., Feger, K.-H., and Schwärzel, K.: Temporal
565 variations of the hydraulic conductivity characteristic under conventional and conservation tillage, GEODERMA, 362,
566 114127, <https://doi.org/10.1016/j.geoderma.2019.114127>, 2020.

567 Leuther, F., Schlüter, S., Wallach, R., and Vogel, H.-J.: Structure and hydraulic properties in soils under long-term irrigation
568 with treated wastewater, GEODERMA, 333, 90–98, <https://doi.org/10.1016/j.geoderma.2018.07.015>, 2019.

569 Van Looy, K., Bouma, J., Herbst, M., Koestel, J., Minasny, B., Mishra, U., Montzka, C., Nemes, A., Pachepsky, Y. A.,
570 Padarian, J., and others: Pedotransfer Functions in Earth System Science: Challenges and Perspectives, REV GEOPHYS, 55,
571 1199–1256, <https://doi.org/10.1002/2017RG000581>, 2017.

572 Metzger, J. C., Filipzik, J., Michalzik, B., and Hildebrandt, A.: Stemflow Infiltration Hotspots Create Soil Microsites Near
573 Tree Stems in an Unmanaged Mixed Beech Forest, FRONT FOR GLOB CHANGE, 4, 701293,
574 <https://doi.org/10.3389/ffgc.2021.701293>, 2021.

575 Moeys, J.: soiltexture: Functions for Soil Texture Plot, Classification and Transformation. R package version 1.5.1.
576 <https://CRAN.R-project.org/package=soiltexture>, 2018.

577 Moshrefi, N.: A new method of sampling soil suspension for particle-size analysis, SOIL SCI., 155, 245–248,
578 <https://doi.org/10.1097/00010694-199304000-00002>, 1993.

579 Mualem, Y.: A New Model for Predicting the Hydraulic Conductivity of Unsaturated Porous Media, WATER RESOUR RES,
580 12, 513–522, <https://doi.org/10.1029/WR012i003p00513>, 1976.

581 Nemes, A., Schaap, M., Leij, F., and Wösten, J.: Description of the unsaturated soil hydraulic database UNSODA version
582 2.0, J HYDROL, 251, 151–162, [https://doi.org/10.1016/S0022-1694\(01\)00465-6](https://doi.org/10.1016/S0022-1694(01)00465-6), 2001.

583 Nemes, A., Wösten, J. H. M., Lilly, A., Oude Voshaar, J.H.: Evaluation of different procedures to interpolate particle-size
584 distributions to achieve compatibility within soil databases. GEODERMA, 90, 187–202, [https://doi.org/10.1016/S0016-7061\(99\)00014-2](https://doi.org/10.1016/S0016-7061(99)00014-2), 1999.

586 Nimmo, J. R.: Comment on the treatment of residual water content in “A consistent set of parametric models for the two-phase
587 flow of immiscible fluids in the subsurface” by L. Luckner et al., WATER RESOUR RES, 27, 661–662,
588 <https://doi.org/10.1029/91WR00165>, 1991.

Formatiert: Schriftfarbe: Schwarz

Formatiert: Standard, Rahmen: Oben: (Kein Rahmen), Unten: (Kein Rahmen), Links: (Kein Rahmen), Rechts: (Kein Rahmen), Zwischen : (Kein Rahmen), Tabstopps: 7,96 cm, Zentriert + 15,92 cm, Rechtsbündig

- 589 Ottoni, M. V., Ottoni Filho, T. B., Schaap, M. G., Lopes-Assad, M. L. R., and Rotunno Filho, O. C.: Hydrophysical Database
590 for Brazilian Soils (HYBRAS) and Pedotransfer Functions for Water Retention, VADOSE ZONE J, 17,
591 https://doi.org/10.2136/vzj2017.05.0095, 2018.
- 592 Pertassek, T., Peters, A., and Durner, W.: HYPROP-FIT software user's manual, V. 3.0, UMS GmbH, Munich, Germany,
593 2015.
- 594 Peters, A.: Simple consistent models for water retention and hydraulic conductivity in the complete moisture range, WATER
595 RESOUR RES, 49, 6765–6780, https://doi.org/10.1002/wrcr.20548, 2013.
- 596 Peters, A. and Durner, W.: Simplified evaporation method for determining soil hydraulic properties, J HYDROL, 356, 147–
597 162, https://doi.org/10.1016/j.jhydrol.2008.04.016, 2008.
- 598 Peters, A. and Durner, W.: SHYPFIT 2.0 User's Manual. Research Report. Institut für Ökologie, Technische Universität
599 Berlin, Germany., 2015.
- 600 Peters, A., Hohenbrink, T. L., Iden, S. C., and Durner, W.: A Simple Model to Predict Hydraulic Conductivity in Medium to
601 Dry Soil From the Water Retention Curve, WATER RESOUR RES, e2020WR029211,
602 https://doi.org/10.1029/2020WR029211, 2021.
- 603 Peters, A., Hohenbrink, T. L., Iden, S. C., Genuchten, M. T. van, and Durner, W.: Prediction of the absolute hydraulic
604 conductivity function from soil water retention data, HYDROL EARTH SYST SC DISCUSSIONS, 2023, 1–32, 27, 1565–
605 1582, https://doi.org/10.5194/hess-2022-43127-1565-2023, 2023.
- 606 R Core Team: R: A Language and Environment for Statistical Computing, R Foundation for Statistical Computing, Vienna,
607 Austria. URL https://www.R-project.org/, 2020.
- 608 Sarkar, S., Germer, K., Maity, R., and Durner, W.: Measuring near-saturated hydraulic conductivity of soils by quasi unit-
609 gradient percolation—1. Theory and numerical analysis, J PLANT NUTR SOIL SC, 182, 524–534,
610 https://doi.org/10.1002/jpln.201800382, 2019a.
- 611 Sarkar, S., Germer, K., Maity, R., and Durner, W.: Measuring near-saturated hydraulic conductivity of soils by quasi unit-
612 gradient percolation—2. Application of the methodology, J PLANT NUTR SOIL SC, 182, 535–540,
613 https://doi.org/10.1002/jpln.201800383, 2019b.
- 614 Schaap, M. G., Leij, F. J., and Van Genuchten, M. T.: ROSETTA: a computer program for estimating soil hydraulic parameters
615 with hierarchical pedotransfer functions, J HYDROL, 251, 163–176, https://doi.org/10.1016/S0022-1694(01)00466-8, 2001.
- 616 Schindler, U.: Ein Schnellverfahren zur Messung der Wasserleitfähigkeit im teilgesättigten Boden an Stechzylinderproben,
617 Arch. Acker- u. Pflanzenbau u. Bodenkdl., Berlin, 24, 1–7, 1980.
- 618 Schindler, U., Durner, W., Von Unold, G., Mueller, L., and Wieland, R.: The evaporation method: Extending the measurement
619 range of soil hydraulic properties using the air-entry pressure of the ceramic cup, J PLANT NUTR SOIL SC, 173, 563–572,
620 https://doi.org/10.1002/jpln.200900201, 2010.
- 621 Schindler, U. G. and Müller, L.: Soil hydraulic functions of international soils measured with the Extended Evaporation
622 Method (EEM) and the HYPROP device, Open Data Journal for Agricultural Research, 3,
623 https://doi.org/10.18174/odjar.v3i1.15763, 2017.

Formatiert: Schriftfarbe: Schwarz

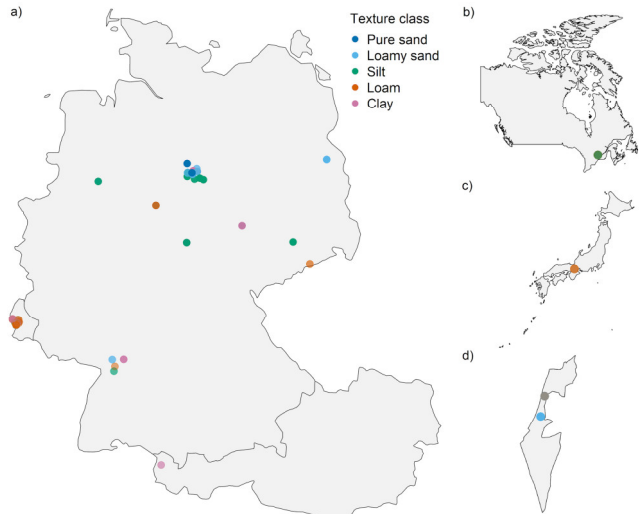
Formatiert: Standard, Rahmen: Oben: (Kein Rahmen), Unten: (Kein Rahmen), Links: (Kein Rahmen), Rechts: (Kein Rahmen), Zwischen : (Kein Rahmen), Tabstopps: 7,96 cm, Zentriert + 15,92 cm, Rechtsbündig

- 624 Schneider, M. and Goss, K.-U.: Prediction of the water sorption isotherm in air dry soils, GEODERMA, 170, 64–69,
 625 https://doi.org/10.1016/j.geoderma.2011.10.008, 2012.
- 626 Tuller, M. and Or, D.: Water films and scaling of soil characteristic curves at low water contents, WATER RESOUR RES, 41,
 627 https://doi.org/10.1029/2005WR004142, 2005.
- 628 [Twarakavi, N. K. C., Šimánek, J., and Schaap, M. G.: Can texture-based classification optimally classify soils with respect to](#)
 629 [soil hydraulics?, Water Resour Res, 46, https://doi.org/10.1029/2009wr007939, 2010.](#)
- 630 [USDA: Soil Taxonomy: A Basic System of Soil Classification for Making and Interpreting Soil Surveys, 2nd edition, United](#)
 631 [States Department of Agriculture, Washington DC, USA, 1999.](#)
- 632 Vereecken, H., Weynants, M., Javaux, M., Pachepsky, Y., Schaap, M., and Genuchten, M. T.: Using Pedotransfer Functions
 633 to Estimate the van Genuchten-Mualem Soil Hydraulic Properties: A Review, VADOSE ZONE J, 9, 795–820,
 634 https://doi.org/10.2136/vzj2010.0045, 2010.
- 635 Weihermüller, L., Lehmann, P., Herbst, M., Rahmati, M., Verhoef, A., Or, D., Jacques, D., and Vereecken, H.: Choice of
 636 Pedotransfer Functions Matters when Simulating Soil Water Balance Fluxes, J ADV MODEL EARTH SY, 13,
 637 e2020MS002404, https://doi.org/10.1029/2020MS002404, 2021.
- 638 Weynants, M., Vereecken, H., and Javaux, M.: Revisiting Vereecken Pedotransfer Functions: Introducing a Closed-Form
 639 Hydraulic Model, VADOSE ZONE J, 8, 86–95, https://doi.org/10.2136/vzj2008.0062, 2009.
- 640 Weynants, M., Montanarella, L., Toth, G., Arnoldussen, A., Anaya Romero, M., Bilas, G., Borresen, T., Cornelis, W.,
 641 Daroussin, J., Gonçalves, M. D. C., and others: European HYdropedological Data Inventory (EU-HYDI), EUR Scientific and
 642 Technical Research Series, https://doi.org/10.2788/5936, 2013.
- 643 Wilkinson, M. D., Dumontier, M., Aalbersberg, I. J., Appleton, G., Axton, M., Baak, A., Blomberg, N., Boiten, J.-W., Silva
 644 Santos, L. B. da, Bourne, P. E., Bouwman, J., Brookes, A. J., Clark, T., Crosas, M., Dillon, I., Dumon, O., Edmunds, S., Evelo,
 645 C. T., Finkers, R., Gonzalez-Beltran, A., Gray, A. J. G., Groth, P., Goble, C., Grethe, J. S., Heringa, J., Hoen, P. A. C. t. Hooft,
 646 R., Kuhn, T., Kok, R., Kok, J., Lusher, S. J., Martone, M. E., Mons, A., Packer, A. L., Persson, B., Rocca-Serra, P., Roos, M.,
 647 Schaijk, R., van Sansone, S.-A., Schulte, E., Sengstag, T., Slater, T., Strawn, G., Swertz, M. A., Thompson, M., Van Der Lei,
 648 J., Van Mulligen, E., Velterop, J., Waagmeester, A., Wittenburg, P., Wolstencroft, K., Zhao, J., and Mons, B.: Comment: The
 649 FAIR Guiding Principles for scientific data management and stewardship, Scientific Data, 3,
 650 https://doi.org/10.1038/sdata.2016.18, 2016.
- 651 Wösten, J., Lilly, A., Nemes, A., and Le Bas, C.: Development and use of a database of hydraulic properties of European soils,
 652 GEODERMA, 90, 169–185, https://doi.org/10.1016/S0016-7061(98)00132-3, 1999.
- 653 Zhang, Y. and Schaap, M. G.: Weighted recalibration of the Rosetta pedotransfer model with improved estimates of hydraulic
 654 parameter distributions and summary statistics (Rosetta3), J HYDROL, 547, 39–53,
 655 https://doi.org/10.1016/j.jhydrol.2017.01.004, 2017.
- 656 Zhang, Y., Weihermüller, L., Toth, B., Noman, M., and Vereecken, H.: Analyzing dual porosity in soil hydraulic properties
 657 using soil databases for pedotransfer function development, VADOSE ZONE J, e20227, https://doi.org/10.1002/vzj2.20227,
 658 2022.

Formatiert: Schriftfarbe: Schwarz
Formatiert: Standard, Rahmen: Oben: (Kein Rahmen), Unten: (Kein Rahmen), Links: (Kein Rahmen), Rechts: (Kein Rahmen), Zwischen : (Kein Rahmen), Tabstopps: 7,96 cm, Zentriert + 15,92 cm, Rechtsbündig

660 **Appendix**

661 Since global coverage and regional distribution of the sampling has not been a criterion for data collection, the samples are
662 basically linked to the research activities of the contributors. Most samples have been taken in Central Europe (n = 508). A
663 few data sets come from Canada (n = 29), Japan (n = 5) and Israel (n = 30) (Figure A1 for visual reference).



664
665
666 **Figure A1:** Locations of the sampling sites in (a) Luxembourg, Germany and Austria, (b) Canada, (c) Japan, and (d) Israel. Please
667 note that the map scales differ, as the maps should only provide a broad overview.

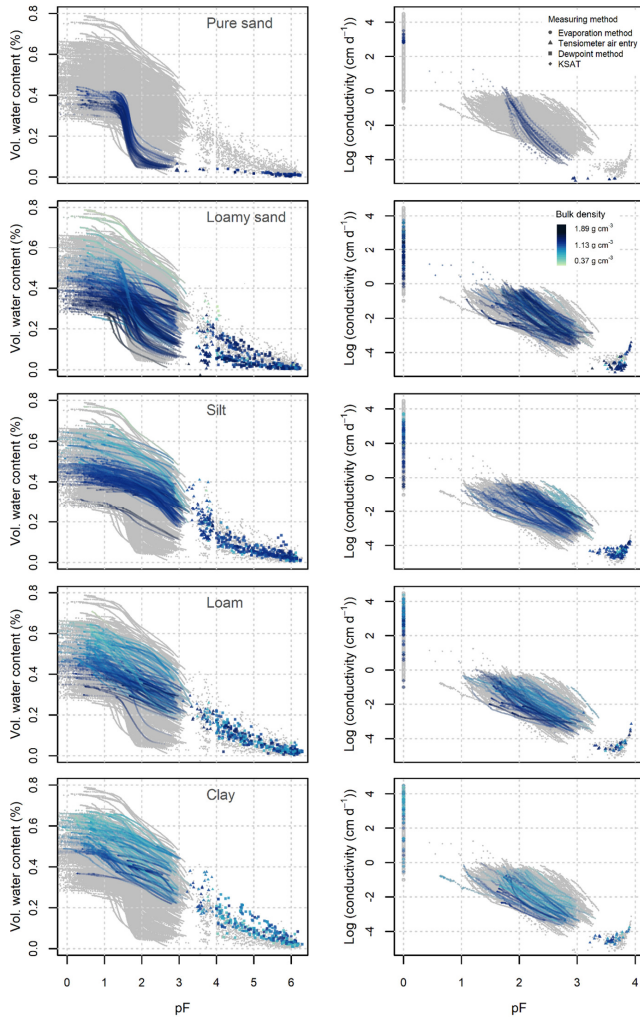
Formatiert: Standard, Abstand Nach: 10 Pt.

Formatiert: Schriftart: 9 Pt., Fett

668
669 Because soil texture classes did not provide strong information about the soil water retention and hydraulic conductivity curves,
670 we have added the same plots as in Figure 3 colour-coded by bulk density (Figure A2).

Formatiert: Schriftfarbe: Schwarz

Formatiert: Standard, Rahmen: Oben: (Kein Rahmen),
Unten: (Kein Rahmen), Links: (Kein Rahmen), Rechts: (Kein Rahmen), Zwischen : (Kein Rahmen), Tabstopps: 7,96 cm,
Zentriert + 15,92 cm, Rechtsbündig



671
 672 **Figure A2:** Soil water retention (left) and hydraulic conductivity (right) colour coded by bulk density. Please note the different pF-
 673 ranges for the retention and conductivity curves. In the online version the different methods contributing to the retention and
 674 conductivity data are plotted as circles (evaporation), triangles (air entry point), squares (dewpoint) and diamonds (K_{sat}).

Formatiert: Abstand Nach: 10 Pt.

Formatiert: Schriftfarbe: Schwarz

Formatiert: Standard, Rahmen: Oben: (Kein Rahmen), Unten: (Kein Rahmen), Links: (Kein Rahmen), Rechts: (Kein Rahmen), Zwischen : (Kein Rahmen), Tabstopps: 7,96 cm, Zentriert + 15,92 cm, Rechtsbündig

| | | |
|--|--------|----------------------------|
| Seite 1: [1] Formatiert | Tobias | 10.07.2023 09:39:00 |
| Schriftfarbe: Schwarz | | |
| Seite 1: [2] Formatiert | Tobias | 10.07.2023 09:39:00 |
| Standard, Rahmen: Oben: (Kein Rahmen), Unten: (Kein Rahmen), Links: (Kein Rahmen), Rechts: (Kein Rahmen), Zwischen : (Kein Rahmen), Tabstopps: 7,96 cm, Zentriert + 15,92 cm, Rechtsbündig | | |
| Seite 1: [3] Formatvorlagendefinition | Tobias | 10.07.2023 09:39:00 |
| Überarbeitung: Block, Zeilenabstand: 1,5 Zeilen | | |
| Seite 1: [4] Formatvorlagendefinition | Tobias | 10.07.2023 09:39:00 |
| Bullets: Mit Gliederung + Ebene: 1 + Nummerierungsformatvorlage: 1, 2, 3, ... + Beginnen bei: 3 + Ausrichtung: Links + Ausgerichtet an: 0 cm + Einzug bei: 0,63 cm | | |
| Seite 1: [5] Formatvorlagendefinition | Tobias | 10.07.2023 09:39:00 |
| Überschrift 5 | | |
| Seite 1: [6] Formatvorlagendefinition | Tobias | 10.07.2023 09:39:00 |
| Überschrift 4 | | |
| Seite 1: [7] Formatvorlagendefinition | Tobias | 10.07.2023 09:39:00 |
| Überschrift 3 | | |
| Seite 1: [8] Formatvorlagendefinition | Tobias | 10.07.2023 09:39:00 |
| Überschrift 2 | | |
| Seite 1: [9] Formatvorlagendefinition | Tobias | 10.07.2023 09:39:00 |
| Standard | | |
| Seite 1: [10] Formatiert | Tobias | 10.07.2023 09:39:00 |
| Schriftart: 17 Pt., Fett, Schriftfarbe: Schwarz, Englisch (Vereinigtes Königreich) | | |
| Seite 1: [11] Formatiert | Tobias | 10.07.2023 09:39:00 |
| Standard, Abstand Vor: 18 Pt., Zeilenabstand: Mehrere 1,83 ze, Rahmen: Oben: (Kein Rahmen), Unten: (Kein Rahmen), Links: (Kein Rahmen), Rechts: (Kein Rahmen), Zwischen : (Kein Rahmen) | | |
| Seite 1: [12] Formatiert | Tobias | 10.07.2023 09:39:00 |
| Vom Text: 0 cm | | |
| Seite 1: [13] Formatiert | Tobias | 10.07.2023 09:39:00 |
| Schriftfarbe: Schwarz | | |
| Seite 1: [14] Formatiert | Tobias | 10.07.2023 09:39:00 |
| Schriftart: 12 Pt., Schriftfarbe: Schwarz | | |
| Seite 1: [15] Formatiert | Tobias | 10.07.2023 09:39:00 |
| Schriftart: 12 Pt., Schriftfarbe: Schwarz, Hochgestellt | | |

| | | |
|--|---------------|----------------------------|
| Seite 1: [16] Formatiert | Tobias | 10.07.2023 09:39:00 |
| Schriftart: 12 Pt., Schriftfarbe: Schwarz | | |
| Seite 1: [17] Formatiert | Tobias | 10.07.2023 09:39:00 |
| Schriftart: 12 Pt., Schriftfarbe: Schwarz | | |
| Seite 1: [18] Formatiert | Tobias | 10.07.2023 09:39:00 |
| Schriftart: 12 Pt., Schriftfarbe: Schwarz | | |
| Seite 1: [19] Formatiert | Tobias | 10.07.2023 09:39:00 |
| Schriftart: 12 Pt., Schriftfarbe: Schwarz | | |
| Seite 1: [20] Formatiert | Tobias | 10.07.2023 09:39:00 |
| Schriftart: 12 Pt., Schriftfarbe: Schwarz | | |
| Seite 1: [21] Formatiert | Tobias | 10.07.2023 09:39:00 |
| Schriftart: 12 Pt., Schriftfarbe: Schwarz | | |
| Seite 1: [22] Formatiert | Tobias | 10.07.2023 09:39:00 |
| Schriftart: 12 Pt., Schriftfarbe: Schwarz | | |
| Seite 1: [23] Formatiert | Tobias | 10.07.2023 09:39:00 |
| Schriftfarbe: Schwarz | | |
| Seite 1: [24] Formatiert | Tobias | 10.07.2023 09:39:00 |
| Deutsch (Deutschland) | | |
| Seite 1: [25] Formatiert | Tobias | 10.07.2023 09:39:00 |
| Standard, Abstand Vor: 6 Pt. | | |
| Seite 1: [26] Formatiert | Tobias | 10.07.2023 09:39:00 |
| Standard, Rahmen: Oben: (Kein Rahmen), Unten: (Kein Rahmen), Links: (Kein Rahmen), Rechts: (Kein Rahmen), Zwischen : (Kein Rahmen) | | |
| Seite 1: [27] Formatiert | Tobias | 10.07.2023 09:39:00 |
| Schriftfarbe: Schwarz, Deutsch (Deutschland) | | |
| Seite 1: [28] Formatiert | Tobias | 10.07.2023 09:39:00 |
| Absatz-Standardschriftart | | |
| Seite 1: [29] Formatiert | Tobias | 10.07.2023 09:39:00 |
| Schriftfarbe: Schwarz | | |
| Seite 1: [30] Formatiert | Tobias | 10.07.2023 09:39:00 |
| Schriftfarbe: Schwarz, Englisch (Vereinigtes Königreich) | | |
| Seite 1: [31] Formatiert | Tobias | 10.07.2023 09:39:00 |

Schriftfarbe: Schwarz

| | | |
|---------------------------------|---------------|----------------------------|
| Seite 1: [32] Formatiert | Tobias | 10.07.2023 09:39:00 |
|---------------------------------|---------------|----------------------------|

Schriftfarbe: Schwarz, Englisch (Vereinigtes Königreich)

| | | |
|---------------------------------|---------------|----------------------------|
| Seite 1: [33] Formatiert | Tobias | 10.07.2023 09:39:00 |
|---------------------------------|---------------|----------------------------|

Schriftfarbe: Schwarz, Englisch (Vereinigtes Königreich)

| | | |
|---------------------------------|---------------|----------------------------|
| Seite 1: [34] Formatiert | Tobias | 10.07.2023 09:39:00 |
|---------------------------------|---------------|----------------------------|

Schriftfarbe: Schwarz, Englisch (Vereinigtes Königreich)

| | | |
|---------------------------------|---------------|----------------------------|
| Seite 1: [35] Formatiert | Tobias | 10.07.2023 09:39:00 |
|---------------------------------|---------------|----------------------------|

Schriftfarbe: Schwarz, Englisch (Vereinigtes Königreich)

| | | |
|---------------------------------|---------------|----------------------------|
| Seite 1: [36] Formatiert | Tobias | 10.07.2023 09:39:00 |
|---------------------------------|---------------|----------------------------|

Schriftfarbe: Schwarz, Englisch (Vereinigtes Königreich)

| | | |
|---------------------------------|---------------|----------------------------|
| Seite 1: [37] Formatiert | Tobias | 10.07.2023 09:39:00 |
|---------------------------------|---------------|----------------------------|

Schriftfarbe: Schwarz, Englisch (Vereinigtes Königreich)

| | | |
|---------------------------------|---------------|----------------------------|
| Seite 1: [38] Formatiert | Tobias | 10.07.2023 09:39:00 |
|---------------------------------|---------------|----------------------------|

Schriftfarbe: Schwarz, Englisch (Vereinigtes Königreich)

| | | |
|---------------------------------|---------------|----------------------------|
| Seite 1: [39] Formatiert | Tobias | 10.07.2023 09:39:00 |
|---------------------------------|---------------|----------------------------|

Schriftfarbe: Schwarz, Englisch (Vereinigtes Königreich)

| | | |
|---------------------------------|---------------|----------------------------|
| Seite 1: [40] Formatiert | Tobias | 10.07.2023 09:39:00 |
|---------------------------------|---------------|----------------------------|

Schriftfarbe: Schwarz